Gut resistome presents a unique biome signature in chronic multi-symptom illness patients and links persistent pro-inflammatory phenotype in a mouse model reversible by fecal microbiota transfer

Dipro Bose
University of South Carolina
Somdatta Chatterjee
University of South Carolina
Ethan Older
University of South Carolina
Ratanesh Seth
University of South Carolina
Patricia Janulewicz Lloyd
Boston University
Jeffrey Carlson
Boston University
Kimberly Sullivan
Boston University
Punnag Saha
University of South Carolina https://orcid.org/0000-0001-6173-9798
Alan Decho
University of South Carolina
Ayan Mondal
University of South Carolina
Jie Li
University of South Carolina https://orcid.org/0000-0001-7977-6749
Nancy Klimas
Institute for Neuro-Immune Medicine
Stephen Lasley
UIC College of Medicine
Saurabh Chatterjee (schatt@mailbox.sc.edu)
University of South Carolina https://orcid.org/0000-0003-1649-7149

Article

Keywords: chronic multi-symptom illness (CMI), gut resistome, fecal microbiota transplant (FMT)

Posted Date: June 22nd, 2021

DOI: https://doi.org/10.21203/rs.3.rs-602469/v1

Version of Record: A version of this preprint was published at Communications Biology on June 7th, 2022. See the published version at https://doi.org/10.1038/s42003-022-03494-7.

Gut resistome presents a unique biome signature in chronic multi-symptom illness patients and links persistent pro-inflammatory phenotype in a mouse model reversible by fecal microbiota transfer

Dipro Bose[1*], Somdatta Chatterjee[1*], Ethan Older[2*], Ratanesh Seth[1], Patricia Janulewicz[3], Punnag Saha[1], Ayan Mondal[1], Jeffrey M. Carlson[3], Alan Decho[1], Kimberly Sullivan[3], Nancy Klimas[4], Stephen Lasley[5], Jie Li[2], Saurabh Chatterjee[1, 6].

Environmental Health and Disease Laboratory, [1]Department of Environmental Health Sciences, Arnold School of Public Health, University of South Carolina, Columbia, SC.

[2]Department of Chemistry and Biochemistry, University of South Carolina, Columbia, SC.

[3]Department of Environmental Health, Boston University School of Public Health, Boston, MA.

[4]Department of Clinical Immunology, Nova Southeastern University, Fort Lauderdale, FL.

[5]Department of Cancer Biology and Pharmacology, University of Illinois college of Medicine, Peoria, IL

[6]Columbia VA Medical Center, Columbia, SC.

[*]Co-first authors with equal contribution.

Abstract:

Chronic multi-symptom illness (CMI) affects a subsection of elderly and war veterans and is associated with systemic inflammation, chronic fatigue, pain and neuroinflammation. We showed previously that an altered gut microbiome-inflammation axis aids to the symptom reporting and persistence. Here, a mouse model of CMI and a group of Gulf War veterans' with CMI showed the presence of an altered host resistome, a signature of antibiotic resistance genes within the microbiome. Results showed that antibiotic resistance genes were significantly altered in the CMI group in both mice and GW veterans when compared to the control. Fecal samples from GW veterans with persistent CMI showed a significant increase of resistance to a wide class of antibiotics and exhibited an array of mobile genetic elements distinct than normal healthy controls. Strikingly, the altered resistome and gene signature were correlated with mouse serum IL6 levels. Altered resistome in mice also correlated strongly with intestinal inflammation, decreased synaptic plasticity that was reversible with fecal microbiota transplant (FMT), a tool to restore a healthy biome. The results indicate an emerging linkage of the gut resistome and CMI and might be significant in understanding the risks to treating hospital acquired infections in this population.

Introduction

Antibiotic resistance has emerged as a threat to public health on the local and global scale [1], [2]. Resistance to antibiotics is conferred on bacteria by antibiotic resistance genes (ARGs). All of the ARGs collectively form a resistome, and usually are carried by the opportunistic pathogens, humans may encounter thus increasing the risk of acquired infection that are difficult to treat with currently approved antibiotics[3], [4], [5], [6]. The evolution of drug resistance in such pathogens is driven by chromosomal mutation and the acquisition of ARGs. Since most of the ARGs are linked to mobile genetic elements (MGEs), they can transfer easily through horizontal gene transfer (HGT) among different clones, taxa and habitats [7], [8], [9], [9], [10].

The human gut harbors multiple commensal microorganisms and forms a good reservoir of ARGs. The gut environment predisposes ARG transfer, sometimes leading to emergence and spread of specific bacterial clones carrying genes of resistance and/or virulence. The most frequently reported genes are those directed against tetracycline, β-lactams, aminoglycosides and glycopeptides. Tetracycline and glycopepetide resistant genes are most common in fecal samples of human [4], [11], [12], [13]. On the other side, human microbiota is also influenced by environmental factors that can contribute to alteration of microbial composition and affect colonization resistance to pathogens [14]. A report from Sun et al., shows that temporary changes in living environment can alter the human gut microbiota and resistome [12]. Another similar study by Parnanen et al. suggested that host also can alter the microbiome and the gut resistome by transmission of ARGs from mother to infant via breast milk [15].

Numerous studies have reported that elderly and war veterans often suffer from multiple syndromes with inflammatory phenotypes and are more susceptible to resistance against

a large number of antibiotics [16], [17], [18]. Veterans have been reported to be resistant to amoxicillin, β-lactams, fluroquinolones, methicillin and most importantly the carbapenem group of antibiotics [19], [20]. In our present study, we aimed to analyze the ARG and mobile genetic element (MGE) patterns in chronic multisymptom illness (CMI) in a GW mouse model as well as in a cohort of GW veterans . GW illness (GWI) is a chronic multisymptomatic illness (CMI) or condition reported by the veterans returning from Operation Desert Storm/Desert Shield in 1991. Symptoms reported by the veterans include fatigue, headache, cognitive dysfunction, musculoskeletal pain, respiratory and gastrointestinal dysfunctions more often characterized by a persistent systemic inflammation with higher IL6, TNF-R1 and IL1β blood levels. These symptoms have been linked to chemical exposures experienced during the war. [21, 22], [23].

Several studies in preclinical mouse models of CMI related to GW have reported that exposure to chemicals such as insecticides and anti-nerve gas resulted in gut microbial dysbiosis. There has been a decrease in the relative abundance of several beneficial bacteria. Recently, a study in GW-CMI veterans also reported similar alteration of gut microbiome [24], [25], [26]. With reported studies on microbial dysbiosis patterns in the preclinical animal models as well as the GW-CMI veteran well established, , we hypothesized that exposure to environmental pesticides and pyridostigmine bromide may also lead to an alteration of ARGs and MGE expression, an important constituent of the gut resistome. In the present study we used both GWI veteran stool samples and fecal pellets from a GWI persistence mouse model mimicking the present day veteran health to study the alteration in gut resistome. We also aimed to study the possible associations between gut resistome and CMI proinflammatory pathology and

mechanistically linked the altered resistome with a proinflammatory phenotype by using a fecal microbiota transfer in mouse models.

Patients/Materials and methods

Permethrin (Per), Pyridostigmine bromide (PB) were purchased from Sigma-Aldrich. Primary antibodies anti-interleukin-1β(IL-1β), anti-brain derived neurotrophic factor (BDNF) were purchased from Santacruz Biotechnology (Dallas, TX, USA).Species specific biotinylated secondary antibodies and streptavidin-HRP (Vectastain ABC Kit) were purchased from Vector laboratories (Burligame,CA,USA). All other chemicals used in the present study were purchased from Sigma unless specified. Animal tissues were sent for paraffin embedding and sectioning to AML Laboratories (Baltimore, MD, USA).Fecal samples from experimental mice groups and GWI veterans were sent to COSMOSID (Rockville, MD, USA) for whole genome sequencing.

Animals

C57BL/6J wild type mice of 10 weeks age were purchased from Jackson Laboratories (BarHarbor, ME, USA). The mice were maintained in accordance with local IACUC standards and National Institute of Health guidelines for human care and use of laboratory animals. All animal experimental procedures were approved by University of South Carolina at Columbia, SC. All the mice had ad libitum access to food and water and were housed at 22-24°C with 12h light/12h dark cycles. The mice were sacrificed after the animal experiments. Organs including frontal cortex and distal part of small intestine were collected after dissecting the mice and fixed in Bouin's solution and 10% neutral buffered formaldehyde respectively. Serum was collected from fresh blood of mice by performing

cardiac puncture after anesthesia. The fecal pellets were collected from colon and it was stored at -80°C for whole-genome sequencing.

Mouse model of CMI related to Gulf War exposures.

After one week of acclimatization, the mice were randomly distributed into three groups. The first group received vehicle (0.6% dimethyl sulfoxide) for two weeks and were denoted Control (n=6). The second and third mice groups denoted GWI(n=6) and GWI_FMT(n=6) were treated with Per (200mg/kg body dissolved in DMSO and phosphate buffer saline(PBS) and PB (2mg/kg dissolved in PBS) by oral gavage tri-weekly for 15 days. After the 2 weeks of GW chemical exposure, GWI group mice were allowed to persist for 20 weeks. Fecal microbiota transplant was administered in GWI_FMT after GW chemical exposure. 100mg of fecal pellets were collected from healthy C57BL/6J mice of same age group as the GWI_FMT mice. The pellets were homogenized in 1ml of PBS and centrifuged at 3000g for 5 min. 100µl of supernatant was dosed in each mice on alternate days of a week for 20 weeks [27].

Human Subjects: GW veterans with CMI and controls

The Boston Gulf War Illness Consortium (GWIC) performs preclinical and clinical studies in order to understand the pathophysiology behind the complex symptoms in GW veterans in order to aid in designing of possible therapeutic strategies. Veterans were included as participants in GWIC studies on the basis of requirement that they had to be deployed in the Gulf War i.e. from August 1990 to July 1991. The GWIC used the Kansas GWI criteria as the case definition which requires the veterans to have symptoms in 3 out of 6 broadly defined group of symptoms (neurological, pain, gastrointestinal, skin,

respiratory, fatigue) to meet criteria of CMI in GW veterans known as Gulf War Illness (GWI)[26],[28]. GW veterans who do not meet Kansas criteria are deemed the control group.

The veterans who participated in the GWIC, underwent multiple tests including neuropsychological asssessments, health surveys, biological specimen collection and brain imaging [22]. The present study was conducted as a GWIC call back study in which we aim to reassess 150 of the GWIC participants. For this study, data from the first 15 recruited subjects from the microbiome call back study has been analyzed. The recruitment of participants was via telephone on completion of GWIC study protocol. After filling out a brief questionnaire regarding screening, the participants were sent a stool collection kit which was then shipped back to the investigators.

Survey Regarding Demographical, Deployment Exposure and Health symptom information

The GWIC participants had to answer to surveys regarding demographics and health condition which included Multi-dimensional Fatigue Inventory (MFI-20), Pittsburg Sleep Quality Index and McGill Pain Inventory [29], [30], [31]. The Structured Neurotoxicant Assessment Checklist (SNAC) and Kansas Gulf War and health Questionnaire and Kansas Gulf War Experiences surveys were given to obtain details about self-reported exposures. The survey regarding health condition provided the details if the participants had an ascertained diagnosis of the medical conditions reported by them [26], [28], [32]. As part of the call back study, the veterans also filled out questionaires about their current and recent gut health and use of antibiotics or probiotics.

Collection of Stool Samples from Participants

The GWIC participants of the microbiome study were mailed a Second Genome stool collection kit (Second Genome, San Francisco, CA, USA). The kit was a self-collecting kit which contained a bar coded vial with stabilizing solution for long term preservation of nucleic acids in stool during transportation and storage. Once received from the subjects, the stool samples were stored at -20°C and upon collection of significant sample numbers, they were sent for whole genome shotgun sequencing by COSMOSID. The protocol was approved by Institutional Review Board at Boston University School of Public Health (proposal no. GW170068) on 4/15/2021.

DNA extraction and Whole Genome Shotgun sequencing

Briefly, the total DNA from mouse and human samples were isolated and purified using ZymoBIOMICS Miniprep kit. DNA was quantified using Qubit dsDNA HS assay (Thermofisher, Waltham, MA,USA). Illumina Nextera XT library preparation kit was used with modifications for preparing DNA libraries. Next generation sequencing (NGS) platform was used to perform whole genome shotgun sequencing (WGS), following protocol optimized by vendor.

Metagenomic analysis and assembly

MetaPhlAn v3.0.7 [33] was used to profile the taxonomic composition of each sample with default parameters. The resulting relative abundance tables were then merged with the provided python tool, “merge_metaphlan_tables.py”. A custom python script was used to filter the data to contain only species level identifications and prepare the operational taxonomic unit (OTU) table for statistical analysis. The metaWRAP v1.3.2 [34] pipeline

was used to process and assemble raw sequencing reads from each sample. First, the "read_qc" module was used with default parameters to trim sequencing adapters and bases with low PHRED scores. To decontaminate the data, reads mapping to the human reference genome GRCh38.p12 (RefSeq Acc: GCF_000001405.38) and the mouse reference genome GRCm38.p6 (RefSeq Acc: GCF_000001635.26) were removed by the metaWRAP "read_qc" module. Decontaminated reads were used for de novo assembly using metaSPAdes [35] as contained in the metaWRAP "assembly" module with default parameters. Resulting contigs were binned by the "binning" module which uses three binning methods, metaBAT2 v2.12.1 [36], MaxBin2 v2.2.6 [37] and CONCOCT v1.0.0 [38] to produce three sets of bins. The "bin_refinement" module was used to refine these three bin sets to produce a single set of best bins. Finally, the single bin set was used by the "bin_reassembly" module which extracts the reads mapping to each bin and uses them for a second round of de novo assembly to improve the completion and reduce the contamination of the bins.

Antimicrobial Resistance Gene Family and MGE Identification.

Contigs produced through metaWRAP were used for open reading frame (ORF) finding using MetaProdigal v2.6.3 [39] with parameters "-c -p meta". ORFs were then clustered with CD-HIT v4.8.1 [40], [41] with parameters "-c 0.95 -s 0.90" corresponding to 95% sequence identity threshold over 90% of the shorter ORF length. Next, ORFs were mapped to the Comprehensive Antibiotic Resistance Database (CARD) v3.1.0 [42] and a recently published custom Mobile Genetic Element (MGE) database composed of 278 distinct genes and over 2000 unique gene sequences [15] using the tool "nhmmer" from the HMMER v3.3.1 [43] software with parameters "-E 0.001 --incE 0.001" corresponding

to an e-value threshold of 0.001 for matches. A custom python script was used to filter multiple hits to select the single best hit for each ORF. Finally, Microsoft Excel was used to generate count data for antimicrobial resistance gene families (AGFs) and MGEs.

Laboratory Methods

Immunohistochemistry

The fixed mouse small intestine and frontal cortex tissues were paraffin embedded and 5 µm thick sections were done for immunohistochemistry. Deparaffinization were performed following previous protocol [44]. Antigen retrieval was performed using epitope retrieval solution and steamer (IHC world, Woodstock, MD, USA). Three percent hydrogen peroxide was used for blocking endogenous peroxidase activity for 20 mins. Serum blocking was performed using 10% goat serum for 1h. Tissue sections were incubated with primary antibodies for IL-1β and BDNF at 1:200 dilution for overnight in humified chamber at 4°C. After incubation, the tissue sections were washed 3 times with PBS containing 0.05% Tween 20 solution. Tissues were probed with species specific biotinylated antibodies (1:200 dilution) followed by incubation with horse radish conjugated streptavidin (1:500 dilution). 3,3'-diaminobenzidine was used as chromogenic substrate solution and counterstaining was performed using Mayer's hematoxylin. The stained tissues sections were mounted using Aqua Mount (Lerner Laboratories, Kalamazoo, MI, USA). The images were acquired using Olympus BX63 microscope (Olympus, Center Valley, PA, USA). Morphometry were performed using Cellsens Software from Olympus America (Centre Valley, PA, USA).

Quantitative RT-PCR

Quantitative RT-PCR (qRT-PCR) was performed to measure ARG expression in DNA extracted from mouse and human stool samples. Gene specific primers were designed using Primer3 (version 0.4.0) and IDT, purchased from Sigma (St. Louis, MO,USA) (Table S1). SYBR Green Supermix (BioRad, Hercules, CA, USA) was used in CFX96 thermal cycler (BioRad, Hercules, CA, USA). The samples (both mouse and human) were run in triplicates for each gene. Ct or threshold cycle values of all ARG genes were normalized with 16S as internal control. $2^{-\Delta\Delta ct}$ method was used to calculate the relative fold change of the ARGs.

ELISA

Serum IL-6 level was estimated using serum collected from the mice groups using commercially available ELISA kit from Proteintech (Rosemont, IL, USA). The ELISA was performed according to the manufacturer's protocol.

Statistical analysis

Analyses were performed using R v3.6.3 (1). AGF, MGE, and OTU count data were normalized based on library size using the "estimateSizeFactors" function from the "DESeq2" package [45] with the parameters "type = poscounts". Normalized count data were then log transformed with the base R function "log2". PERMANOVA was calculated using the "adonis" function from the package "vegan" (2) with Bray-Curtis dissimilarity and 9999 permutations. Welch two-sample t-test was implemented using the base R function "t.test" with the parameters "conf.level = 0.95, alternative = two.sided" indicating 95% confidence level and two-tailed testing. PCA ordinations of AGF and Taxonomy abundance data were performed using the "rda" function from "vegan". Procrustes

analysis was performed using PCA ordinations with the function “protest” from “vegan” with 9999 permutations. Distance-based redundancy analysis was performed with the “capscale” function from the “vegan” package with Bray-Curtis dissimilarity. Unpaired *t*-tests (two-tailed tests with equal variance) were performed followed by Bonferroni-Dunn post-hoc analysis to compare between the mouse experimental groups and veteran groups respectively. Chao1 α-diversity was calculated using the “chao1” function from the “fossil” package. Correlation analyses between α-diversity and selected biomarkers were performed using Pearson’s correlation implemented by the base R function “cor”. All visualizations were rendered using the “ggplot2” package unless otherwise described. For all analyses, $p \leq 0.05$ was considered statistically significant and data are represented as mean ± standard error of mean.

Results

Characterization of Anti-microbial resistance in mouse fecal samples

We performed whole genome shotgun sequencing, metagenomic assembly, and functional gene annotation on fecal samples collected from 3 groups: Control, GWI, and GWI_FMT) to construct AGF profiles associated with the GWI mouse model and the fecal microbiota transplant FMT treatment. We detected 95 unique AGFs with an even distribution across all groups with 185 ± 4 (mean ± standard error) total AGFs in Control, 182 ± 3 total AGFs in GWI, and 188 ± 4 total AGFs in GWI_FMT (Fig. 1a). We used permutational multivariate analysis of variance (PERMANOVA) to compare the AGF profiles between sample groups which revealed a significant deviation between the GWI_FMT and GWI ($R^2 = 42.2\%$, $p = 0.002$) and GWI_FMT and Control groups ($R^2 = 41.3\%$, $p = 0.0001$). This analysis indicates that the sample group variable explains

roughly 40% of the variation in the resistome profile. To get a clearer picture of the specific changes in the resistome, we performed differential abundance analysis of the AGFs by manually selecting the AGFs with the greatest variance in relative abundance between sample groups and compared their sum relative abundance as a subset of the resistome (Fig. 1b). These selected AGF groups were significantly increased in the GWI group when compared to the Control group (Welch two-sample t-test, $p = 0.004134$) and between the GWI and GWI_FMT groups (Welch two-sample t-test, $p = 0.00008972$). To explain these changes, we performed procrustes rotation of the principal component analyses (PCAs) of the resistome and microbiome profiles which showed a significant correlation between resistome changes and microbiome composition changes (PROTEST, $M^2 = 0.2834$, $p = 0.0001$, Fig. 1c). Further, distance-based redundancy analysis showed clear segregation of the AGF profiles of each group with that of the GWI_FMT group lying between the Control and GWI groups in the CAP2 axis suggesting that FMT treatment may act to return the resistome to a more Control-like state (Fig. 1D).

To assess the transferability of the AGFs in the microbiome, we also examined the profile of the MGEs constituting the mobilome in each sample group. We detected 67 unique MGEs evenly distributed across all groups with 74 ± 5 total MGEs in Control, 71 ± 3 total MGEs in GWI, and 80 ± 3 total MGEs in GWI_FMT (Fig. 1e). PERMANOVA showed that significant differences in the mobilomes of the GWI_FMT and GWI groups ($R^2 = 42.9\%$, $p = 0.0022$) and the GWI_FMT and Control groups ($R^2 = 30.6\%$, $p = 0.0024$). The relative abundance of manually selected MGEs were also significantly different between Control and GWI groups (Welch two-sample t-test, $p = 0.002101$) and between the GWI and GWI_FMT groups (Welch two-sample t-test, $p = 0.0003543$).

290 Distribution of ARGs and MGEs across different mouse groups

291 In our analysis of the gut resistome, we detected multiple genes AFGs imparting
292 resistance to antimicrobial classes which have been, marked as highly important and
293 critically important by the World Health Organization WHO (AGISAR, 2018). Overall,
294 glycopepetide resistance genes were the most common type of AGF followed by
295 quinolones, polymyxins and carbapenem resistance genes. The relative abundance of
296 vancomycin resistance genes were highest (4.44% van-R, 3.57% van-S, 2.33% van-Y
297 and 1.9% van-T) in GWI group compared to Control and GWI_FMT groups (Fig 2a).
298 Interestingly, there were 38 unique genes which were only present in the GWI group but
299 not in the Control or GWI_FMT groups. Of these genes, mcr-1 and ndm-1 drew the most
300 concern because of their high transferability. The Control group also showed maximum
301 resistance towards vancomycin followed by RND (resistance nodulation cell division)
302 efflux pump, MATE transporter and β-lactamase resistance genes. Apart from
303 vancomycin-methicillin resistance, resistance against penicillin, cephalosporins, and
304 macrolides were also observed in GWI_FMT samples. Though these mice were not
305 exposed to any of these antibiotics, and the very fact that they showed resistance towards
306 members of critically important the highest priority group of antimicrobials (AGISAR,
307 2018,WHO) is a matter of concern.

308 When comparing the different drug class resistance across the three groups, the majority
309 of the resistome was composed of genes imparting mixed resistance against drug classes
310 with the largest single class being glycopeptide resistance. Genes against this drug class
311 consisted of 4.6% and, 4.4%, and 3.83% of the GWI, Control, and GWI_FMT resistome
312 respectively. Apart from the observed glycopeptide resistance, other similar fractions of

313 the resistomes detected were in relation to macrolide antibiotics with 4.14%, 4.08%, and
314 3.74% respectively, peptide antibiotics with 4.06%, 3.94%, and 3.45% respectively,
315 tetracycline antimicrobials 4.08%, 4.01%, and 3.75% respectively and nitroimidazole
316 antibiotics which were present 3.76%, 3.63%, and 3.12% respectively in the GWI, control
317 and GWI_FMT groups (Fig 2b). Multivariate analysis of the profiles of drug class
318 resistances showed significant deviation and correlation dependent on sample groups
319 when comparing the GWI_FMT and Control groups (PERMANOVA, R^2 = 40.9%, p =
320 0.0027) and the GWI_FMT and GWI groups (PERMANOVA, R^2 = 56.4%, p = 0.0025).
321 Typical gene signatures are identifiable for classes of resistance mechanisms.
322 Resistance mechanism genes such as those which are known to be associated with
323 antibiotic efflux were identified and and made up the highest percentage of all resistomes
324 (20.33%, 20.15%, 19.75% in GWI, control and GWI_FMT respectively) (Fig 2c). Other
325 mechanisms of resistance included target alteration, target protection, and antibiotic
326 inactivation as well as target replacement. When calculating the percentages of these
327 mechanisms, GWI group had the highest value of abundance when compared to the
328 other groups namely, control and GWI+FMT.

329 We then investigated the presence of different MGEs and MGE types among all of the
330 samples. As ARGs have high propensity to transfer from one bacteria to another, the
331 evaluation of different MGE elements is of utmost importance. Tnp A was most the
332 predominant mobile genetic element present in GWI group followed by IS 91, int2, ISCrspI
333 and intI1 (Fig2d). When comparing different types of MGEs, transposases was found to
334 be the highest in terms of abundance and counts(14.5% in GWI, 14.2% in control and
335 11.8% in GWI_FMT). Tn 916 (9.3% in GWI), integrase (11.2% in GWI), ISCR (9.57%)

were also present in all the 3 groups of mice (Fig 2e). Multivariate analysis of the MGE type profiles showed a significant deviation and correlation pattern that was dependent on sample groups when comparing to the GWI_FMT and Control groups (PERMANOVA, R^2 = 42.2%, p = 0.0024) and the GWI_FMT and GWI groups (PERMANOVA, R^2 = 52.2%, p = 0.0018).

Characterization of anti-microbial resistance gene in human samples

In order to study whether the results observed on our mouse model were mirrored in the human subjects, we obtained 15 stool samples from GWI veterans (5 in the Hum_Control group and 10 the in Hum_GWI group). We then performed whole genome shotgun sequencing, metagenomic assembly, and functional gene annotation. We detected 108 unique AGFs with 175 ± 3 and 182 ± 3 total occurrences in the Control group and GWI groups respectively (Fig 3a). On comparing the relative abundance of AGFs, we observed a modest but insignificant deviation in the resistome profiles between the two groups (PERMANOVA, R^2 = 7.2%, p = 0.4428). When looking at a more granular scale, there was an insignificant decrease in the relative abundance of selected AGFs (Welch two-sample t-test, p = 0.6874) (Fig 3b). Procustes analysis showed a significant correlation of bacterial taxa and the AGFs (PROTEST, M^2 = 0.5972, p = 0.004) (Fig 3c). Despite minor divergence indicated by multivariate analysis, distance-based redundancy analysis showed clear clustering of the control and GWI groups with minimal overlap on the first two constrained principal coordinates (Fig 3d).

Looking at transferability, we identified 92 unique MGEs across both groups with 77 ± 5 and 85 ± 3 total MGEs in the Control group and the GWI groups respectively (Fig 3e). While there was some deviation in the MGE profiles of the two groups, multivariate

analysis revealed that these changes were not significantly dependent on the sample groups (PERMANOVA, R^2 = 6.5%, p = 0.599). Interestingly, the relative abundance of selected MGEs were higher in GWI group compared to the Control, however, this difference was not statistically significant (Welch two-sample t-test, p = 0.05331) (Fig 3f).

Distribution of selected ARGs and MGEs in human samples

To check the distribution of ARGs and MGEs in human samples, identical analysis was carried out in the 2 groups of human data. Ciprofloxacin antibiotic efflux pump showed the highest relative abundance in GWI (5.26%) followed by RND antibiotic efflux pump (4.16% in GWI), vanR (3.96% in GWI) and tetR (3.65% in GWI) (Fig 4a).

Comparing the drug class resistances of the 2 groups, glycopeptide antibiotic was most predominant followed by macrolide, tetracycline, fluroquinolone and glycycline antibiotics. The percentage of the resistance were observed in the sequence of 4.08%, 4.01%, 3.91% and 3.1% respectively. The profiles of drug class resistances did not significantly deviate or depend on the sample group (PERMANOVA, R^2 = 6.4%, p = 0.6181) (Fig 4b)

A total 9 different types of resistance mechanisms were detected, in which antibiotic efflux pump (20.72 % in GWI and 20.76% in control) was the most common. The mechanisms of antibiotic target alteration, protection, inactivation and replacement mechanisms were also detected across the 2 groups (Fig 4c).

Among the 31 unique different MGE groups studied, tnp A was found to be most predominant (7.8% in GWI, 8.8% in Control). A total of 23 MGEs were found to be present in the GWI group. Int2, IS 91, IS 621 and MGE 10 were found to be present in both groups (Fig 4d). We also observed 8 different MGE types unique in GWI group but

transposases (13.63% in GWI and 12.71% in control) and integrases (10.67% in GWI and 9.97% in control) were found to be the most abundant in all MGE types (Fig 4e). Multivariate analysis of the MGE class profiles revealed moderate deviation between sample groups which was shown to be independent when compared between sample groups (PERMANOVA, R^2 = 12.1%, p = 0.0632).

Expression study of antimicrobial resistance genes in mouse and GWI veteran samples by q-RTPCR analysis

Based on the host microbial genome analysis in the mouse model we selected 13 different resistant genes when compared between mouse GWI and mouse Control (AGF count cut off value-1), 19 different resistant genes when compared between mouse GWI and mouse GWI_FMT (AGF count cut off value 1) and 10 when compared between GWI-veteran and control-veterans (AGF count cut off value-3).

The expression of VANU gene was 6 fold higher in GWI mouse group when compared to the mouse control group. The rifampin phosphotransferase (RP) gene also showed a 6 fold increase in mouse GWI group followed by AAC3' (5.56 fold), NDM (4.45 fold), APH6 (3.6 fold), MCRK (2.66 fold), MCRE (2.3 fold) when compared to subsequent controls. The estimation of the expression of resistant genes against mouse GWI and GWI_FMT groups revealed that AAC3' expression was highest with fold change of 7.23 when compared to the FMT group. OXA β-lactamase (OXA) also showed fold change of 4.5, while FONA β-lactamase (FONA) showed a change of 3.15 fold when compared to the FMT group. Subsequently, the expression of BAH amidohydrolase (BAH) and class C LRA β-lactamase (LRA) were increased by 3.1 and 2.15 fold when compared to FMT

groups suggesting that fecal microbiota transfer was efficient in decreasing the abundance and expression of these antimicrobial resistance genes(Fig 5a & b).

Comparison of microbiome sequencing data in human samples showed that there was a huge increase in expression of isolucyl t RNA synthetase (ILES) (267 fold), phospho-ethanolamine transferase (PMR) (162 fold), RND efflux pump (RND) (82 fold) followed by rifamycin resistant (RPOB) and chloramphenicol acetyl-transferase (CAT) (37 fold) in the GWI group when compared to controls suggesting that the present day Gulf war veteran with CMI had a significant alteration of antibiotic resistance pattern when compared to controls (Fig 5c).

Gastrointestinal, systemic and neuronal inflammation and its association with ARGs and Drug Classes in mouse GW-CMI samples

Gastrointestinal and neuronal inflammation is reported in deployed GW veterans with CMI also termed as GWI and in preclinical GW-CMI mouse models due to the influence of GW chemicals ([26], [46], [47], [48], [49], [50]. Increase in systemic inflammatory markers were also reported in GWI veterans and mouse models [51], [26], [50], [52]. Following our study of the expression of AGFs and MGEs, we focused our study to examine whether an association exists between AGFs and MGEs and biomarkers of GWI pathology thus suggesting a role of gut resistome in influencing the host health. The purpose was also to show whether a predictive insight can be made to future susceptibility to infectious disease related to hospital acquired infections in the veterans, elderly and immunocompromised individuals. Results in mice showed that the expression of IL-1β in small intestine significantly increased in GWI group ($p<0.000001$) compared to the Control group, as shown by immunoreactivity of the cytokine in the villi (Fig 6a,b).

Treatment with FMT significantly decreased ($p<0.000001$) the expression of IL-1β in GWI_FMT mice groups compared to GW group (Fig 6a,B). To study the association between IL-1β expression and AGF diversity, we performed a correlation analysis. Results showed a positive correlation ($r= 0.8463$, $p=0.034$ & $r=0.9691$, $p=0.001$ respectively) between α-diversity of AGFs, resistant drug classes and IL-1β, suggesting that alteration of gut resistome had a significant correlation in gastrointestinal inflammation (Fig 6f).

We observed a significant increase ($p=0.000413$) in serum IL-6 level in GWI mouse group when compared to Control and GWI_FMT group (Fig 6c). Results also suggested that increased α-diversity of AGFs and resistant drug classes positively correlated ($r=0.8043$, $p=0.196$ & $r=0.9669$, $p=0.033$) with increased systemic IL-6 level in GW mouse group (Fig 6g).

Our previous studies have reported that a decrease in synaptic plasticity marker BDNF played a key role in brain pathology in GW chemical exposed mice [44] Results showed that expression of BDNF significantly decreased ($p=<0.00001$ between Control vs GWI & GWI vs GWI_FMT) in GWI group when compared to Control and GW_FMT mice groups (Fig 6d). Interestingly, a negative correlation ($r=-0.8866$, $p=0.19$ & $r=-0.9799$, $p<0.001$) was observed between BDNF and AGFs suggesting that increased AGF-α-diversity may have a strong influence on observed neuroinflammation GWI mice group (Fig 6j)

Discussion

We report a novel alteration of host gut resistome in chronic multisymptom illness as observed in a subsection of Gulf War veterans. We also linked the association of systemic inflammation and an altered gut resistome that is linked to increased circulating proinflammatory cytokine IL6, intestinal pathology and neurotrophic factor BDNF. IL6 has been shown to be a pleiotropic cytokine and is key to gastrointestinal disturbances, and cognitive deficits [53], [54]. Recent advances in understanding the host resistome improved our knowledge about evolution, origins and emergence of antibiotic resistance though the field is still evolving [55]. Previously, our knowledge of resistome included proto-resistance and silent resistance genes [55]. Silent-resistance genes do not cause phenotypic resistance until they are transferred via MGEs or a mutation occurs in the associated regulatory elements. Gut microbiome is usually associated with a silent resistome, as they have the potential to contribute in clinical resistance through mobilization [55]. Changes in the host environment has a direct effect on human microbiome that leads to the enrichment of ARGs [12, 56]. Association to MGEs increases the susceptibility to antibiotic resistance of the host gut microbiome. Sun et al., reported that the gut microbiome and resistome of veterinary students visiting a swine farm had been significantly altered after their 3 months visit which was partially restored even after 4-6 months post visit [12]. A recent report suggested that COVID-19-associated travel norms had greater impact on gut microbiota and ARGs than did pre-pandemic international travel [57]. As a result, the phylum *Actinobacteria*, known to be a resident of the gut, decreases while the resistance against β-lactams, polystyrene increases thus impacting the gut physiology [57]. Our study supports the existing evidence that the resistome is highly dependent on the gut microbiome and proves a strong association

between changes in the bacterial taxa and the gut resistome, particularly in GWI groups, both in the case of mouse models and veterans with GWI as studied by PERMANOVA and procustes analysis. Interestingly, we found that the richness of ARGs increases with the GW chemical exposure early in the life cycle.

Previous reports stated that elderly individuals and veterans had increased resistance to sulfonamide, macrolide, β-lactam antibiotics followed by tetracycline as well as fluoroquinolones especially found in *Acinetobacter baumannii* isolates [58], [59] . Reports also stated that fluoroquinolones and cephalosporin usage should be prescribed in a limited manner among the elderly and veterans as they have higher susceptibility in developing resistances upon treatment with such high generation antibiotics [59]. However, there is very little evidence about the ARGs in veterans, especially GW veterans suffering from CMI or collectively referred as GWI who were deployed 30 years back and are presently in the age range of 50-60 years. The present study is the first to report the alteration of ARG signature in GW-CMI veterans as well as in preclinical CMI mouse model closely related to GW which mimics the present health condition of the GW-CMI veterans. We identified that glycopeptide resistance is high in GWI compared to other mouse groups following macrolide, peptide and tetracycline antibiotics. This study also suggests that GW chemical exposure may be responsible for the alteration and appearance of ARGs and MGEs in mice since they have been maintained in a controlled environment with very few risk of exposure to a multifaceted environment. A further study of the resistant drug classes as well as mechanisms of resistance showed that antibiotic efflux is the major mechanism of resistance in both mouse and GW-CMI veterans. The

493 above mechanism further aids the transfer of the glycopeptide antibiotic efflux and may
494 act as a signature resistance mechanisms associated with GW-CMI pathology.

495 FMT has been reported to restore the beneficial microbiome in pathological conditions
496 like irritable bowel syndrome, type 2 diabetes, nonalcoholic steatohepatitis, neurological
497 disorders and type 2 diabetes where gut microbial dysbiosis plays a direct role in the
498 disease progression [60], [61]. Studies have also reported that FMT administration have
499 decreased the ARGs in patients with cirrhosis and *Clostridium difficile* infection[61]. In
500 the present study, we treated GW chemical exposed mice with FMT in GWI_FMT group.
501 We observed a significant decrease in relative abundance of selected AGFs and MGEs
502 in GWI_FMT. Moreover, the results showed an increase in unique AGFs and MGEs in
503 GWI_FMT which may be transferred from the resident commensal microbiome of the
504 donor mice group. This also emphasizes the need for screening the fecal samples of
505 healthy donors for FMT [62].

506 One of the important highlights of this study is the accumulation of ARGs in GW-chronic
507 multisymptom illness group that have high transferable capacity. This transfer may occur
508 through horizontal gene transfer (HGT) method based on MGE patterns. *MCR*
509 *phosphoethanolamine transferase* and *NDM beta-lactamase* are two such the genes that
510 are present in GWI mouse group but not in Control and GWI_ FMT group. As mentioned
511 previously, these mice were never exposed to any kind of antibiotics (β-lactams or
512 colistin) during the entire course of the study, but they showed a spontaneous acquisition
513 of AGFs in GW chemical exposed group. This may be due to intrinsic transfer or extrinsic
514 transfer through HGT. We were able to confirm the presence of these genes by
515 sequencing (data not shown), but further studies are needed to study their mechanism of

transfer. Another limitation in our observation of gene transfer may be from the use of diet in these mice. The mice in our study were fed with the standard chow diet though in a consistent manner in all groups. Diet induced acquisition of microbial resistance genes should be studied as a mechanism of acquiring antibiotic resistance genes in all further studies though the chemical exposure was the principal variable that differentiated the groups.

Here in this study, we were able to identify diverse types of MGEs in which *tnpA* is most abundant followed by transposase. Another study by Parnanen et al. stated that transposase constitute most abundant MGE class in all samples [15]. This study completely is consistent with our observations about MGEs. Higher abundance of MGEs belonging to transposon group indicated that there is a higher potential for ARG transfer in GW-CMI pathology. To track the ARG transfer through MGE, detailed investigation is needed whether these genes can transfer through any transferrable plasmids or by any other IS element/ transposons.

Studies have also reported that low dose antibiotics have increased the abundance of a single pathogenic bacteria, however, difference in ARGs were not significant compared to control groups [63]. This study also showed change in immunological markers but association between ARGs and immunological markers have not been established [63]. Also, IBD phenotype is known to be associated with microbiome dysbiosis which led to upregulation of antibiotic resistance [64], a condition also observed in GW-CMI veterans [65]. We have shown a direct association between gastrointestinal, systemic and neuronal inflammation observed in GW-CMI pathology and diversity of AGFs and resistant drug classes in a mouse model. Interestingly, association between diversity of

AGFs and systemic proinflammatory marker IL-6 will be an important benchmark in future studies of chronic multisymptom illness and other related pathology. Further, mechanistic studies are needed to establish the exact role of ARGs in GWI pathophysiology and can be aided by GW-CMI veterans studies where probiotics or microbiome restoring short chain fatty acids (butyrate) is used as a therapy.

In conclusion, our study revealed for the first time that exposure to GW chemicals associated with CMI caused significant changes in ARGs and MGEs in GW-CMI mouse model and veterans alike. Further , a strong association was stablished between an altered resistome and systemic IL6 levels in a translatable mouse model that has broad implications in the general population suffering from similar ailments. Strikingly it is expected that a strong 78 million of the US population will be elderly category by 2030. Most of them have a history of prolonged antibiotic use, a case similar with our aging veterans. The scenario is also striking owing to old age associated hospitalizations and increased chances of hospital acquired infections. In addition, FMT can be used as a therapeutic strategy against the increased antibiotic resistance in veterans and elderly to attenuate a possible altered resistome. A focused study on each of the antibiotic resistant genes that was altered in the CMI mouse model and its modulation by FMT or in GW-CMI veterans can be an avenue for drug discovery and personalized medicine in future.

Conflict of Interest

The authors declare no conflict of interest.

Acknowledgement

We are grateful to the Instrument Resource Facility (University of South Carolina School of Medicine) and AML Labs (Baltimore, MD, USA) for providing excellent technical service. We would also like to thank COSMOSID (Microbial Genomic Platform, Rockville, MD, USA) for their valuable assistance in whole genome shotgun sequencing. We acknowledge Dr. Dao-Peng Chen (Kim Forest Enterprise Co., Ltd.) and Dr. Zhenjiang Zech Xu (State Key Laboratory of Food Science and Technology, Nanchang University) for providing sequence coding consultation and assistance.

Author contributions:

Conceptualization:, S.C.; experimentation: DB, SDC, EO, PS, RS; data curation:, DB, SDC, EO, JL, SC, PJ, KS; formal analysis: DB, SDC, EO; funding acquisition:, S.C.; investigation, methodology, resources:, S.C,.; R.S. , A.M., P.S.,; D.B., SDC, EO ; software:, DB, SDC, EO; supervision:, S.C., R.S., J.L; writing—original draft:, DB, SDC, EO and S.C.; writing: S.C.; review and editing: S.C., N.K.,; K.S.,; P.J.,; S.L.,;A.D. All authors have read and agreed to the published version of the manuscript .

Funding:

This study was supported by DoD-IIRFA Grant W81XWH1810374 to Saurabh Chatterjee, W81XWH-13-2-0072 to Kim Sullivan. and VA Merit Award I01CX001923-01 to Dr. Saurabh Chatterjee. Partially supported by a National Science Foundation EPSCoR Program OIA-1655740 to Dr. Jie Li.

This work was supported in part by a Merit Review Award I01CX001923-01 from the United States (U.S.) Department of Veterans Affairs Clinical Sciences Research and Development Service

Disclaimer: The contents do not represent the views of the U.S. Department of Veterans Affairs or the United States Government.

Data availability and resources: Microbiome and resistome sequence data that support the findings of this study have been deposited in GenBank with the accession code : PRJNA734321 with the link: https://www.ncbi.nlm.nih.gov/sra/PRJNA734321

References:

1. Sabtu N, Enoch DA and Brown NM (2015) Antibiotic resistance: what, why, where, when and how? Br Med Bull 116:105-13. doi: 10.1093/bmb/ldv041
2. Bengtsson B and Greko C (2014) Antibiotic resistance--consequences for animal health, welfare, and food production. Ups J Med Sci 119:96-102. doi: 10.3109/03009734.2014.901445
3. Munita JM and Arias CA (2016) Mechanisms of Antibiotic Resistance. Microbiol Spectr 4. doi: 10.1128/microbiolspec.VMBF-0016-2015
4. Singh S, Verma N and Taneja N (2019) The human gut resistome: Current concepts & future prospects. Indian J Med Res 150:345-358. doi: 10.4103/ijmr.IJMR_1979_17
5. Wright GD (2010) The antibiotic resistome. Expert Opin Drug Discov 5:779-88. doi: 10.1517/17460441.2010.497535
6. Crofts TS, Gasparrini AJ and Dantas G (2017) Next-generation approaches to understand and combat the antibiotic resistome. Nat Rev Microbiol 15:422-434. doi: 10.1038/nrmicro.2017.28
7. McInnes RS, McCallum GE, Lamberte LE and van Schaik W (2020) Horizontal transfer of antibiotic resistance genes in the human gut microbiome. Curr Opin Microbiol 53:35-43. doi: 10.1016/j.mib.2020.02.002
8. Lerminiaux NA and Cameron ADS (2019) Horizontal transfer of antibiotic resistance genes in clinical environments. Can J Microbiol 65:34-44. doi: 10.1139/cjm-2018-0275
9. Partridge SR, Kwong SM, Firth N and Jensen SO (2018) Mobile Genetic Elements Associated with Antimicrobial Resistance. Clin Microbiol Rev 31. doi: 10.1128/CMR.00088-17
10. Stokes HW and Gillings MR (2011) Gene flow, mobile genetic elements and the recruitment of antibiotic resistance genes into Gram-negative pathogens. FEMS Microbiol Rev 35:790-819. doi: 10.1111/j.1574-6976.2011.00273.x
11. Martin D (1992) Operating laparoscopes. Nursing (Lond) 5:27-30.
12. Sun J, Liao XP, D'Souza AW, Boolchandani M, Li SH, Cheng K, Luis Martinez J, Li L, Feng YJ, Fang LX, Huang T, Xia J, Yu Y, Zhou YF, Sun YX, Deng XB, Zeng ZL, Jiang HX, Fang BH, Tang YZ, Lian XL, Zhang RM, Fang ZW, Yan QL, Dantas G and Liu YH (2020) Environmental remodeling of human gut microbiota and antibiotic resistome in livestock farms. Nat Commun 11:1427. doi: 10.1038/s41467-020-15222-y

13. van Schaik W (2015) The human gut resistome. Philos Trans R Soc Lond B Biol Sci 370:20140087. doi: 10.1098/rstb.2014.0087
14. Phillips ML (2009) Gut reaction: environmental effects on the human microbiota. Environ Health Perspect 117:A198-205. doi: 10.1289/ehp.117-a198
15. Parnanen K, Karkman A, Hultman J, Lyra C, Bengtsson-Palme J, Larsson DGJ, Rautava S, Isolauri E, Salminen S, Kumar H, Satokari R and Virta M (2018) Maternal gut and breast milk microbiota affect infant gut antibiotic resistome and mobile genetic elements. Nat Commun 9:3891. doi: 10.1038/s41467-018-06393-w
16. Fitzpatrick MA, Suda KJ, Safdar N, Burns SP, Jones MM, Poggensee L, Ramanathan S and Evans CT (2018) Changes in bacterial epidemiology and antibiotic resistance among veterans with spinal cord injury/disorder over the past 9 years. J Spinal Cord Med 41:199-207. doi: 10.1080/10790268.2017.1281373
17. Jones BE, Jones MM, Huttner B, Stoddard G, Brown KA, Stevens VW, Greene T, Sauer B, Madaras-Kelly K, Rubin M, Goetz MB and Samore M (2015) Trends in Antibiotic Use and Nosocomial Pathogens in Hospitalized Veterans With Pneumonia at 128 Medical Centers, 2006-2010. Clin Infect Dis 61:1403-10. doi: 10.1093/cid/civ629
18. Kelly AA, Jones MM, Echevarria KL, Kralovic SM, Samore MH, Goetz MB, Madaras-Kelly KJ, Simbartl LA, Morreale AP, Neuhauser MM and Roselle GA (2017) A Report of the Efforts of the Veterans Health Administration National Antimicrobial Stewardship Initiative. Infect Control Hosp Epidemiol 38:513-520. doi: 10.1017/ice.2016.328
19. Fitzpatrick MA, Suda KJ, Poggensee L, Vivo A, Wirth M, Wilson G, Evans M and Evans CT (2021) Epidemiology and clinical outcomes associated with extensively drug-resistant (XDR) Acinetobacter in US Veterans' Affairs (VA) medical centers. Infect Control Hosp Epidemiol 42:305-310. doi: 10.1017/ice.2020.450
20. Wilson BM, El Chakhtoura NG, Patel S, Saade E, Donskey CJ, Bonomo RA and Perez F (2017) Carbapenem-Resistant Enterobacter cloacae in Patients from the US Veterans Health Administration, 2006-2015. Emerg Infect Dis 23:878-880. doi: 10.3201/eid2305.162034
21. White RF, Steele L, O'Callaghan JP, Sullivan K, Binns JH, Golomb BA, Bloom FE, Bunker JA, Crawford F, Graves JC, Hardie A, Klimas N, Knox M, Meggs WJ, Melling J, Philbert MA and Grashow R (2016) Recent research on Gulf War illness and other health problems in veterans of the 1991 Gulf War: Effects of toxicant exposures during deployment. Cortex 74:449-75. doi: 10.1016/j.cortex.2015.08.022
22. Janulewicz P, Krengel M, Quinn E, Heeren T, Toomey R, Killiany R, Zundel C, Ajama J, O'Callaghan J, Steele L, Klimas N and Sullivan K (2018) The Multiple Hit Hypothesis for Gulf War Illness: Self-Reported Chemical/Biological Weapons Exposure and Mild Traumatic Brain Injury. Brain Sci 8. doi: 10.3390/brainsci8110198
23. Mawson AR and Croft AM (2019) Gulf War Illness: Unifying Hypothesis for a Continuing Health Problem. Int J Environ Res Public Health 16. doi: 10.3390/ijerph16010111
24. Alhasson F, Das S, Seth R, Dattaroy D, Chandrashekaran V, Ryan CN, Chan LS, Testerman T, Burch J, Hofseth LJ, Horner R, Nagarkatti M, Nagarkatti P, Lasley SM and Chatterjee S (2017) Altered gut microbiome in a mouse model of Gulf War Illness causes neuroinflammation and intestinal injury via leaky gut and TLR4 activation. PLoS One 12:e0172914. doi: 10.1371/journal.pone.0172914
25. Seth RK, Kimono D, Alhasson F, Sarkar S, Albadrani M, Lasley SK, Horner R, Janulewicz P, Nagarkatti M, Nagarkatti P, Sullivan K and Chatterjee S (2018) Increased butyrate priming in the gut stalls microbiome associated-gastrointestinal inflammation and hepatic metabolic reprogramming in a mouse model of Gulf War Illness. Toxicol Appl Pharmacol 350:64-77. doi: 10.1016/j.taap.2018.05.006
26. Janulewicz PA, Seth RK, Carlson JM, Ajama J, Quinn E, Heeren T, Klimas N, Lasley SM, Horner RD, Sullivan K and Chatterjee S (2019) The Gut-Microbiome in Gulf War Veterans: A Preliminary Report. Int J Environ Res Public Health 16. doi: 10.3390/ijerph16193751

27. Yan Y, Zhou X, Guo K, Zhou F and Yang H (2020) Chlorogenic Acid Protects Against Indomethacin-Induced Inflammation and Mucosa Damage by Decreasing Bacteroides-Derived LPS. Front Immunol 11:1125. doi: 10.3389/fimmu.2020.01125
28. Steele L (2000) Prevalence and patterns of Gulf War illness in Kansas veterans: association of symptoms with characteristics of person, place, and time of military service. Am J Epidemiol 152:992-1002. doi: 10.1093/aje/152.10.992
29. Smets EM, Garssen B, Bonke B and De Haes JC (1995) The Multidimensional Fatigue Inventory (MFI) psychometric qualities of an instrument to assess fatigue. J Psychosom Res 39:315-25. doi: 10.1016/0022-3999(94)00125-o
30. Melzack R (1975) The McGill Pain Questionnaire: major properties and scoring methods. Pain 1:277-299. doi: 10.1016/0304-3959(75)90044-5
31. Buysse DJ, Reynolds CF, 3rd, Monk TH, Berman SR and Kupfer DJ (1989) The Pittsburgh Sleep Quality Index: a new instrument for psychiatric practice and research. Psychiatry Res 28:193-213. doi: 10.1016/0165-1781(89)90047-4
32. Proctor SP, Heeren T, White RF, Wolfe J, Borgos MS, Davis JD, Pepper L, Clapp R, Sutker PB, Vasterling JJ and Ozonoff D (1998) Health status of Persian Gulf War veterans: self-reported symptoms, environmental exposures and the effect of stress. Int J Epidemiol 27:1000-10. doi: 10.1093/ije/27.6.1000
33. Beghini F, McIver LJ, Blanco-Miguez A, Dubois L, Asnicar F, Maharjan S, Mailyan A, Manghi P, Scholz M, Thomas AM, Valles-Colomer M, Weingart G, Zhang Y, Zolfo M, Huttenhower C, Franzosa EA and Segata N (2021) Integrating taxonomic, functional, and strain-level profiling of diverse microbial communities with bioBakery 3. Elife 10. doi: 10.7554/eLife.65088
34. Uritskiy GV, DiRuggiero J and Taylor J (2018) MetaWRAP-a flexible pipeline for genome-resolved metagenomic data analysis. Microbiome 6:158. doi: 10.1186/s40168-018-0541-1
35. Nurk S, Meleshko D, Korobeynikov A and Pevzner PA (2017) metaSPAdes: a new versatile metagenomic assembler. Genome Res 27:824-834. doi: 10.1101/gr.213959.116
36. Kang DD, Li F, Kirton E, Thomas A, Egan R, An H and Wang Z (2019) MetaBAT 2: an adaptive binning algorithm for robust and efficient genome reconstruction from metagenome assemblies. PeerJ 7:e7359. doi: 10.7717/peerj.7359
37. Wu YW, Simmons BA and Singer SW (2016) MaxBin 2.0: an automated binning algorithm to recover genomes from multiple metagenomic datasets. Bioinformatics 32:605-7. doi: 10.1093/bioinformatics/btv638
38. Alneberg J, Bjarnason BS, de Bruijn I, Schirmer M, Quick J, Ijaz UZ, Lahti L, Loman NJ, Andersson AF and Quince C (2014) Binning metagenomic contigs by coverage and composition. Nat Methods 11:1144-6. doi: 10.1038/nmeth.3103
39. Hyatt D, Chen GL, Locascio PF, Land ML, Larimer FW and Hauser LJ (2010) Prodigal: prokaryotic gene recognition and translation initiation site identification. BMC Bioinformatics 11:119. doi: 10.1186/1471-2105-11-119
40. Li W and Godzik A (2006) Cd-hit: a fast program for clustering and comparing large sets of protein or nucleotide sequences. Bioinformatics 22:1658-9. doi: 10.1093/bioinformatics/btl158
41. Fu L, Niu B, Zhu Z, Wu S and Li W (2012) CD-HIT: accelerated for clustering the next-generation sequencing data. Bioinformatics 28:3150-2. doi: 10.1093/bioinformatics/bts565
42. Alcock BP, Raphenya AR, Lau TTY, Tsang KK, Bouchard M, Edalatmand A, Huynh W, Nguyen AV, Cheng AA, Liu S, Min SY, Miroshnichenko A, Tran HK, Werfalli RE, Nasir JA, Oloni M, Speicher DJ, Florescu A, Singh B, Faltyn M, Hernandez-Koutoucheva A, Sharma AN, Bordeleau E, Pawlowski AC, Zubyk HL, Dooley D, Griffiths E, Maguire F, Winsor GL, Beiko RG, Brinkman FSL, Hsiao WWL, Domselaar GV and McArthur AG (2020) CARD 2020: antibiotic resistome surveillance with the comprehensive antibiotic resistance database. Nucleic Acids Res 48:D517-D525. doi: 10.1093/nar/gkz935

43. Potter SC, Luciani A, Eddy SR, Park Y, Lopez R and Finn RD (2018) HMMER web server: 2018 update. Nucleic Acids Res 46:W200-W204. doi: 10.1093/nar/gky448
44. Bose D, Saha P, Mondal A, Fanelli B, Seth RK, Janulewicz P, Sullivan K, Lasley S, Horner R, Colwell RR, Shetty AK, Klimas N and Chatterjee S (2020) Obesity Worsens Gulf War Illness Symptom Persistence Pathology by Linking Altered Gut Microbiome Species to Long-Term Gastrointestinal, Hepatic, and Neuronal Inflammation in a Mouse Model. Nutrients 12. doi: 10.3390/nu12092764
45. Love MI, Huber W and Anders S (2014) Moderated estimation of fold change and dispersion for RNA-seq data with DESeq2. Genome Biol 15:550. doi: 10.1186/s13059-014-0550-8
46. Broderick G, Kreitz A, Fuite J, Fletcher MA, Vernon SD and Klimas N (2011) A pilot study of immune network remodeling under challenge in Gulf War Illness. Brain Behav Immun 25:302-13. doi: 10.1016/j.bbi.2010.10.011
47. Alshelh Z, Albrecht DS, Bergan C, Akeju O, Clauw DJ, Conboy L, Edwards RR, Kim M, Lee YC, Protsenko E, Napadow V, Sullivan K and Loggia ML (2020) In-vivo imaging of neuroinflammation in veterans with Gulf War illness. Brain Behav Immun 87:498-507. doi: 10.1016/j.bbi.2020.01.020
48. Seth RK, Maqsood R, Mondal A, Bose D, Kimono D, Holland LA, Janulewicz Lloyd P, Klimas N, Horner RD, Sullivan K, Lim ES and Chatterjee S (2019) Gut DNA Virome Diversity and Its Association with Host Bacteria Regulate Inflammatory Phenotype and Neuronal Immunotoxicity in Experimental Gulf War Illness. Viruses 11. doi: 10.3390/v11100968
49. Hernandez S, Fried DE, Grubisic V, McClain JL and Gulbransen BD (2019) Gastrointestinal neuroimmune disruption in a mouse model of Gulf War illness. FASEB J 33:6168-6184. doi: 10.1096/fj.201802572R
50. Kimono D, Bose D, Seth RK, Mondal A, Saha P, Janulewicz P, Sullivan K, Lasley S, Horner R, Klimas N and Chatterjee S (2020) Host Akkermansia muciniphila Abundance Correlates With Gulf War Illness Symptom Persistence via NLRP3-Mediated Neuroinflammation and Decreased Brain-Derived Neurotrophic Factor. Neurosci Insights 15:2633105520942480. doi: 10.1177/2633105520942480
51. Butterick TA, Trembley JH, Hocum Stone LL, Muller CJ, Rudquist RR and Bach RR (2019) Gulf War Illness-associated increases in blood levels of interleukin 6 and C-reactive protein: biomarker evidence of inflammation. BMC Res Notes 12:816. doi: 10.1186/s13104-019-4855-2
52. Bose D, Mondal A, Saha P, Kimono D, Sarkar S, Seth RK, Janulewicz P, Sullivan K, Horner R, Klimas N, Nagarkatti M, Nagarkatti P and Chatterjee S (2020) TLR Antagonism by Sparstolonin B Alters Microbial Signature and Modulates Gastrointestinal and Neuronal Inflammation in Gulf War Illness Preclinical Model. Brain Sci 10. doi: 10.3390/brainsci10080532
53. Pawlowska-Kamieniak A, Krawiec P and Pac-Kozuchowska E (2021) Interleukin 6: Biological significance and role in inflammatory bowel diseases. Adv Clin Exp Med 30:465-469. doi: 10.17219/acem/130356
54. Wright CB, Sacco RL, Rundek T, Delman J, Rabbani L and Elkind M (2006) Interleukin-6 is associated with cognitive function: the Northern Manhattan Study. J Stroke Cerebrovasc Dis 15:34-8. doi: 10.1016/j.jstrokecerebrovasdis.2005.08.009
55. Perry JA, Westman EL and Wright GD (2014) The antibiotic resistome: what's new? Curr Opin Microbiol 21:45-50. doi: 10.1016/j.mib.2014.09.002
56. Foster KR, Schluter J, Coyte KZ and Rakoff-Nahoum S (2017) The evolution of the host microbiome as an ecosystem on a leash. Nature 548:43-51. doi: 10.1038/nature23292
57. Peng Y, Zhang D, Chen T, Xia Y, Wu P, Seto WK, Kozyrskyj AL, Cowling BJ, Zhao J and Tun HM (2021) Gut microbiome and resistome changes during the first wave of the COVID-19 pandemic in comparison with pre-pandemic travel-related changes. J Travel Med. doi: 10.1093/jtm/taab067
58. Modak R, Ross D and Kan VL (2008) Macrolide and clindamycin resistance in Staphylococcus aureus isolates and antibiotic use in a Veterans Affairs Medical Center. Infect Control Hosp Epidemiol 29:180-2. doi: 10.1086/526448

59. Livorsi DJ, Suda KJ, Cunningham Goedken C, Hockett Sherlock S, Balkenende E, Chasco EE, Scherer AM, Goto M, Perencevich EN, Goetz MB and Reisinger HS (2021) The feasibility of implementing antibiotic restrictions for fluoroquinolones and cephalosporins: a mixed-methods study across 15 Veterans Health Administration hospitals. J Antimicrob Chemother. doi: 10.1093/jac/dkab138
60. Khoruts A and Sadowsky MJ (2016) Understanding the mechanisms of faecal microbiota transplantation. Nat Rev Gastroenterol Hepatol 13:508-16. doi: 10.1038/nrgastro.2016.98
61. Vindigni SM and Surawicz CM (2017) Fecal Microbiota Transplantation. Gastroenterol Clin North Am 46:171-185. doi: 10.1016/j.gtc.2016.09.012
62. Woodworth MH, Carpentieri C, Sitchenko KL and Kraft CS (2017) Challenges in fecal donor selection and screening for fecal microbiota transplantation: A review. Gut Microbes 8:225-237. doi: 10.1080/19490976.2017.1286006
63. Hu Q, Liu C, Zhang D, Wang R, Qin L, Xu Q, Che L and Gao F (2020) Effects of Low-Dose Antibiotics on Gut Immunity and Antibiotic Resistomes in Weaned Piglets. Front Immunol 11:903. doi: 10.3389/fimmu.2020.00903
64. Xia Y, Wang J, Fang X, Dou T, Han L and Yang C (2021) Combined analysis of metagenomic data revealed consistent changes of gut microbiome structure and function in inflammatory bowel disease. J Appl Microbiol. doi: 10.1111/jam.15154
65. Keating JA, Shaughnessy C, Baubie K, Kates AE, Putman-Buehler N, Watson L, Dominguez N, Watson K, Cook DB, Rabago D, Suen G, Gangnon R and Safdar N (2019) Characterising the gut microbiome in veterans with Gulf War Illness: a protocol for a longitudinal, prospective cohort study. BMJ Open 9:e031114. doi: 10.1136/bmjopen-2019-031114

Figure Legends:

Fig. 1 Distribution of ARGs and MGEs in mouse models. a. Boxplots showing total abundance of antimicrobial gene families (AGFs) in Control (wild type mice administered with vehicle, n=6), GWI (GW chemical exposed persistence mice group, n=6) and GWI_FMT(persistent mice group exposed to GW chemicals followed by FMT treatment, n=6). Boxes indicate interquartile range (n=6 biologically independent in each group). Median values of 187 in Control, 185 in GWI, and 190 in GWI_FMT indicated by solid black lines. Error bars extend to the most extreme values within 1.5 time the interquartile range. Differences between mean total AGFs detected shown to be insignificant (Control – GWI p = 0.557, GWI – GWI_FMT p = 0.312) by Welch two sample *t*-test. **b.** Comparison of the relative abundance (%) of selected AGFs between (**i**) GWI and Control groups and (**ii**) GWI and GWI_FMT groups. **c.** Procrustes rotation analysis comparing resistome (blue) and microbiome (red) changes using PCA ordinations, (X axis: PCA1, PCA2-Y axis,

PROTEST, M^2 = 0.2834, P= 0.0001). **d.** dbRDA of Bray-Curtis dissimilarity between ARG and Taxa across sample groups. Constrained principal co-ordinates CAP1 (35.6 %) and CAP2 (4.2 %) are calculated to explain 39.8 % of variance detected. L ines connect points from the center of gravity of each sample group. **e.** Boxplot of total abundance of MGEs with median values 72 in Control, 72 in GWI, and 80 in GWI_FMT. **f.** Relative abundance (%) of selected mobile genetic elements (MGEs) **i.** Control and GWI, **ii.** GWI and GWI_FMT

Fig. 2 Classification of selected AGFs and MGEs. a. Group bar chart showing relative abundance (%) of selected AGFs in Control, GWI, and GWI_FMT. Stacked bar analysis of relative abundance (%) of **b.** drug classes resistances and **c.** mechanisms of resistance. Relative abundance (%) of **d.** MGEs and **e.** MGE types.

Fig. 3 Distribution of AGFs and MGEs in GWI-veteran groups. a. Change in total abundance of AGFs in Hum_Control (veteran group without GWI symptom, n=5) and Hum_GWI (veteran group with GWI symptom, n=10) with median values of 177 in Hum_Control and 181 in Hum_GWI. Differences in total abundance values were shown to be insignificant (p = 0.1001) by Welch two-sample *t*-test. **b.** Comparison of relative abundance (%) of selected AGFs between Hum_Control and Hum_GWI groups. **c.** Procrustes rotation analysis comparing resistome (blue) and microbiome (red) changes using PCA ordinations, (X axis: PCA1, PCA2-Y axis, PROTEST, M^2 = 0.5972, P= 0.0028). **d.** dbRDA of Bray-Curtis dissimilarity between AGFs and Taxa. Constrained principal co-ordinates CAP1-(6.5 %) and CAP2 (18.6 %) account for variance 25.1 % of detected variance. **e.** Total abundance of MGE element with median values 80 in Hum_Control and 85 in Hum_GWI. **f.** Relative abundance (%) of selected MGEs in Hum_Control and Hum_GWI

Fig. 4 Classification of selected AGFs and MGEs in veterans. a Grouped bar chart showing relative abundance (%) of AGFs in Hum_Control and Hum_GWI. **b** Stacked bar analysis of

relative abundance (%) of **b**. drug classes and **c.** mechanisms of resistance. Relative abundance (%) of **d.** MGEs and **e.** MGE types.

Fig. 5 Relative expression levels of antimicrobial resistance genes: mRNA expression of AGFs **a.** Between Control and GWI **b.** Between GWI and GWI_FMT **c.** Between Hum_Control and Hum_GWI groups. The mRNA expression was calculated as fold change against control (in 5a), against GWI_FMT (in 5b) and Hum_Control (in 5c). All data are represented as mean ± SEM. Statistical significance was analysed using unpaired T-test where *p<0.05, **p<0.01, ***p<0.001.

Fig. 6 **Gastrointestinal, systemic, brain inflammation and its correlation with antibiotic resistance genes and the drug classes in GWI mouse model.** (a)Representative immunohistochemistry image showing immunoreactivity of proinflammatory cytokine IL-1β (marked by red circle) in Control (wild type mice administered with vehicle, n=6), GWI (GW chemical exposed persistence mice group, n=6) and GWI_FMT(persistent mice group exposed to GW chemicals followed by FMT treatment, n=6). Images were taken at 20X magnification. (b) Bar graph depicting immunoreactivity of IL-1β. Results are represented as mean±SD of %ROI (mean value calculated from 2 different fields in each sample). Statistical significance was analyzed by unpaired t-test where *p<0.05, **p<0.01, ***p<0.001. (c) Bar graph depicting the serum IL-6 level at pg/ml in Control, GWI, GWI_FMT mice groups. Statistical significance was analyzed by unpaired t-test where *p<0.05, **p<0.01, ***p<0.001. (d) Representative immunohistochemistry image showing immunoreactivity of synaptic plasticity marker BDNF (marked by red arrows) in Control, GWI, GWI_FMT mice groups. Images were taken at 20X magnification. FC - Frontal Cortex, HC – Hippocampus. (e) Bar graph depicting immunoreactivity of BDNF. Results are represented as mean±SD of %ROI (mean value calculated from 2 different fields in each sample). Statistical significance was analyzed by unpaired t-test where *p<0.05, **p<0.01, ***p<0.001. (f) Correlation plot between α-diversity (Chao1) of resistant AGFs and drug classes and immunoreactivity of IL-1β in mouse GW group in small intestine section. Pearson's

linear regression is shown in red with 95% confidence bands. (g) Correlation plot between α-diversity (Chao1) of resistant AGFs and drug classes and serum IL-6 level in mouse GW group. Pearson's linear regression is shown in red with 95% confidence bands.(h) Correlation plot between α-diversity (Chao1) of resistant AGFs and drug classes and immunoreactivity of BDNF in mouse GW group in brain section. Pearson's linear regression is shown in red with 95% confidence bands.

Fig. 1

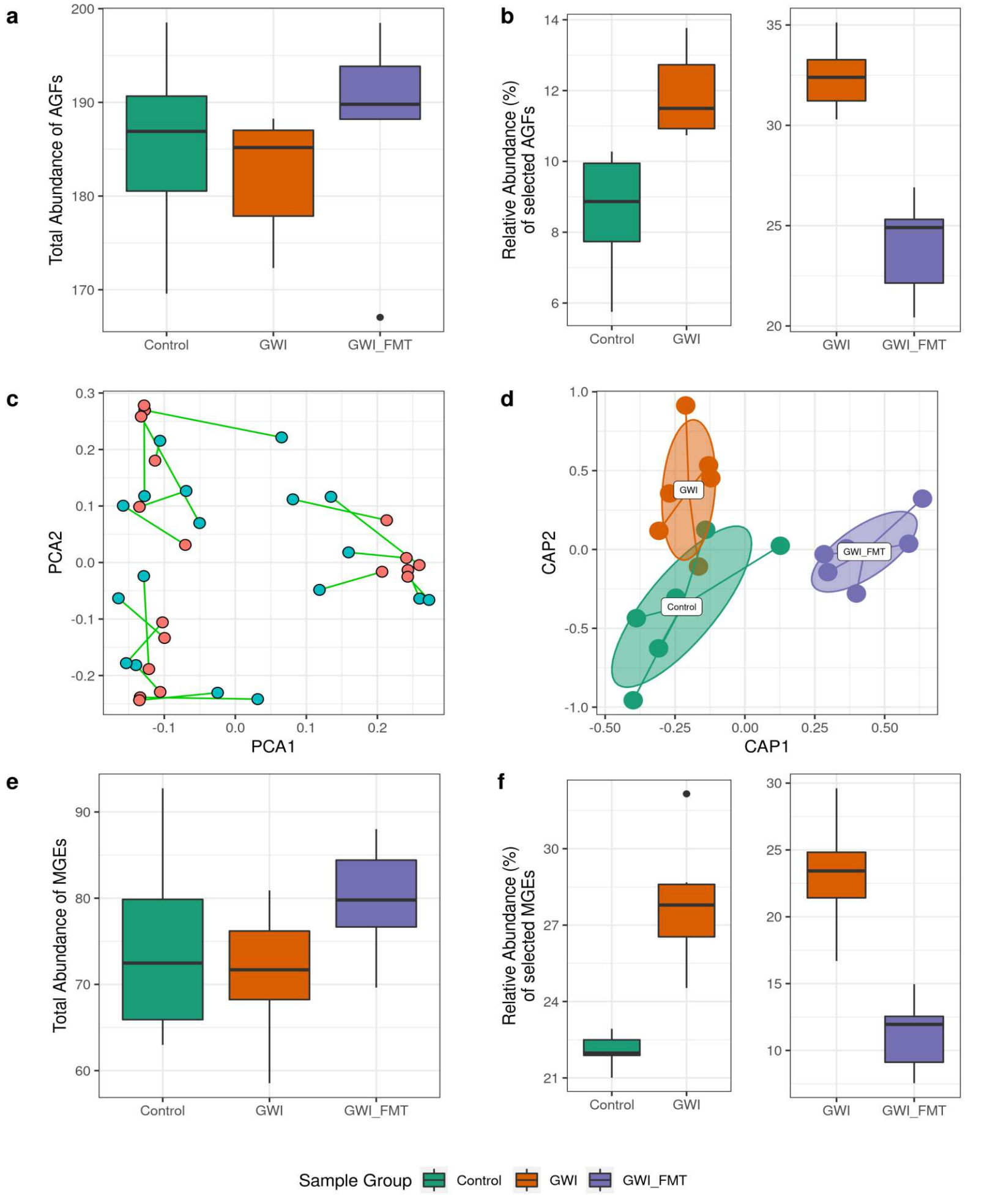
a
Total Abundance of AGFs
200
190
180
170
Control
GWI
GWI_FMT
b
Relative Abundance (%) of selected AGFs
14
12
10
8
6
Control
GWI
35
30
25
20
GWI
GWI_FMT
c
PCA2
0.3
0.2
0.1
0.0
-0.1
-0.2
-0.1
0.0
0.1
0.2
PCA1
d
CAP2
1.0
0.5
0.0
-0.5
-1.0
GWI
GWI_FMT
Control
-0.50
-0.25
0.00
0.25
0.50
CAP1
e
Total Abundance of MGEs
90
80
70
60
Control
GWI
GWI_FMT
f
Relative Abundance (%) of selected MGEs
30
27
24
21
Control
GWI
30
25
20
15
10
GWI
GWI_FMT
Sample Group
Control
GWI
GWI_FMT

Fig. 2

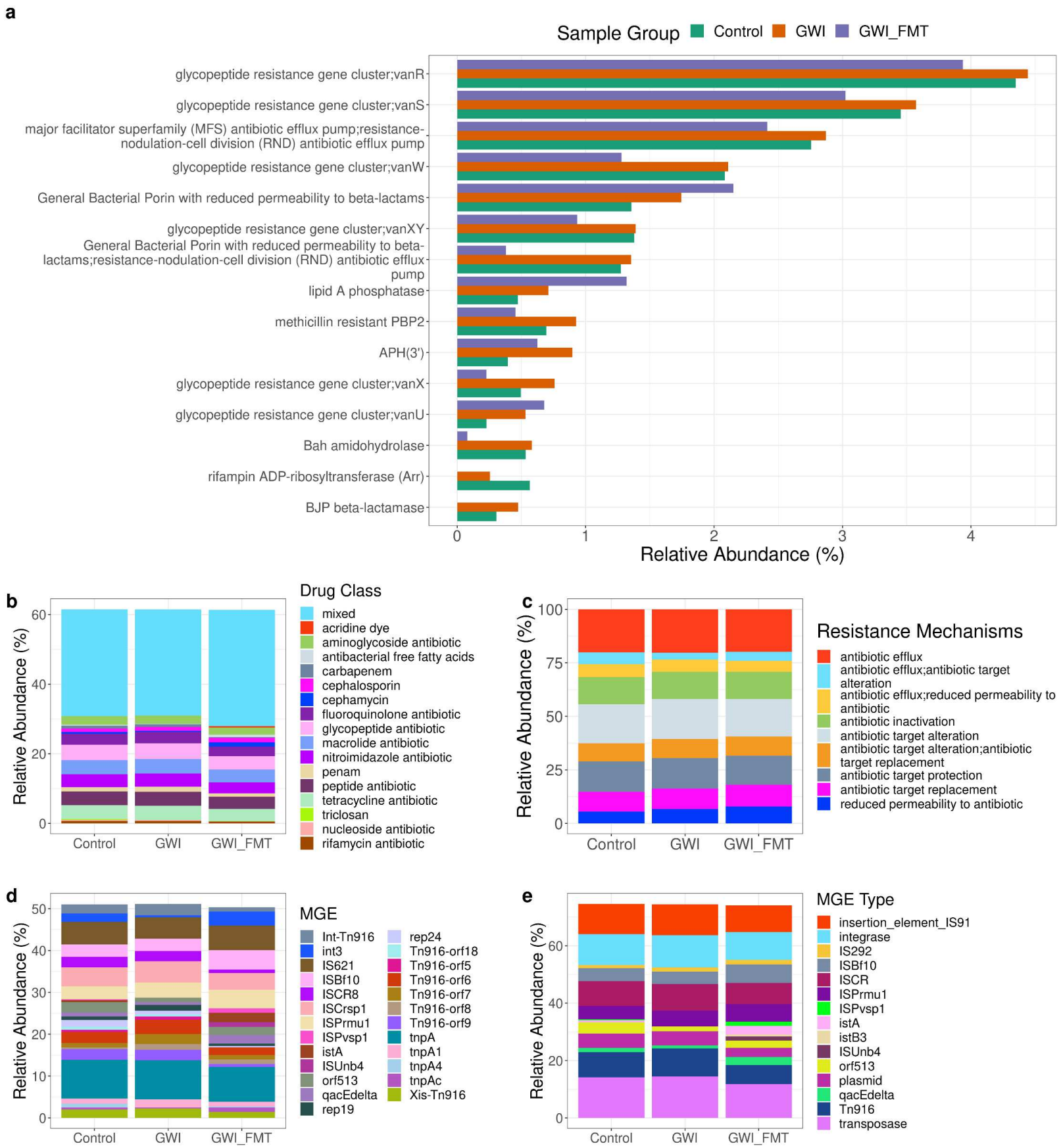
a
Sample Group
Control
GWI
GWI_FMT
glycopeptide resistance gene cluster;vanR
glycopeptide resistance gene cluster;vanS
major facilitator superfamily (MFS) antibiotic efflux pump;resistance-nodulation-cell division (RND) antibiotic efflux pump
glycopeptide resistance gene cluster;vanW
General Bacterial Porin with reduced permeability to beta-lactams
glycopeptide resistance gene cluster;vanXY
General Bacterial Porin with reduced permeability to beta-lactams;resistance-nodulation-cell division (RND) antibiotic efflux pump
lipid A phosphatase
methicillin resistant PBP2
APH(3')
glycopeptide resistance gene cluster;vanX
glycopeptide resistance gene cluster;vanU
Bah amidohydrolase
rifampin ADP-ribosyltransferase (Arr)
BJP beta-lactamase
0
1
2
3
4
Relative Abundance (%)
b
Relative Abundance (%)
Control
GWI
GWI_FMT
Drug Class
mixed
acridine dye
aminoglycoside antibiotic
antibacterial free fatty acids
carbapenem
cephalosporin
cephamycin
fluoroquinolone antibiotic
glycopeptide antibiotic
macrolide antibiotic
nitroimidazole antibiotic
penam
peptide antibiotic
tetracycline antibiotic
triclosan
nucleoside antibiotic
rifamycin antibiotic
c
Relative Abundance (%)
Resistance Mechanisms
antibiotic efflux
antibiotic efflux;antibiotic target alteration
antibiotic efflux;reduced permeability to antibiotic
antibiotic inactivation
antibiotic target alteration
antibiotic target alteration;antibiotic target replacement
antibiotic target protection
antibiotic target replacement
reduced permeability to antibiotic
d
Relative Abundance (%)
MGE
Int-Tn916
int3
IS621
ISBf10
ISCR8
ISCrsp1
ISPrmu1
ISPvsp1
istA
ISUnb4
orf513
qacEdelta
rep19
rep24
Tn916-orf18
Tn916-orf5
Tn916-orf6
Tn916-orf7
Tn916-orf8
Tn916-orf9
tnpA
tnpA1
tnpA4
tnpAc
Xis-Tn916
e
Relative Abundance (%)
MGE Type
insertion_element_IS91
integrase
IS292
ISBf10
ISCR
ISPrmu1
ISPvsp1
istA
istB3
ISUnb4
orf513
plasmid
qacEdelta
Tn916
transposase

Fig. 3

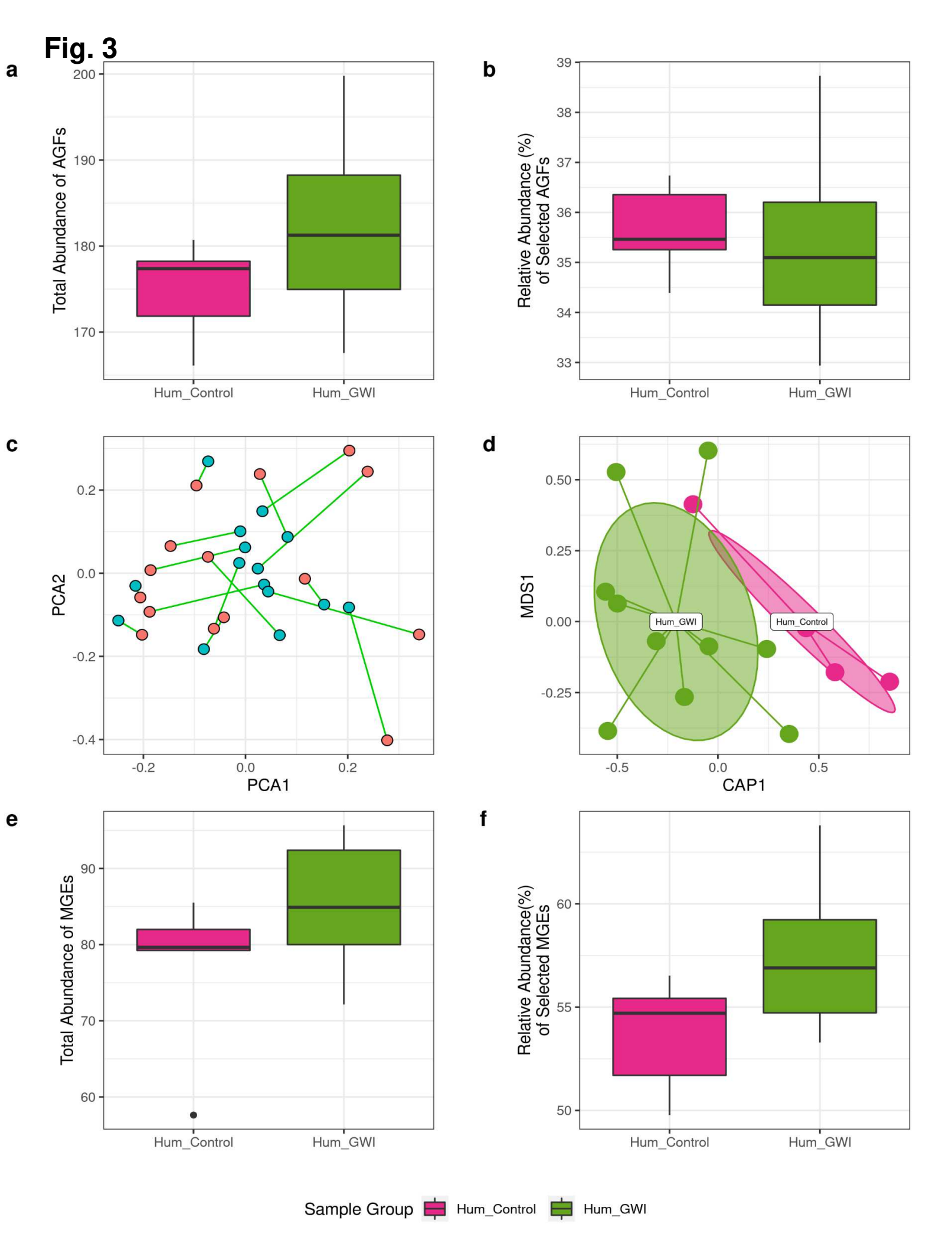
a
Total Abundance of AGFs
200
190
180
170
Hum_Control
Hum_GWI
b
Relative Abundance (%)
of Selected AGFs
39
38
37
36
35
34
33
Hum_Control
Hum_GWI
c
PCA2
0.2
0.0
-0.2
-0.4
-0.2
0.0
0.2
PCA1
d
MDS1
0.50
0.25
0.00
-0.25
Hum_GWI
Hum_Control
-0.5
0.0
0.5
CAP1
e
Total Abundance of MGEs
90
80
70
60
Hum_Control
Hum_GWI
f
Relative Abundance(%)
of Selected MGEs
60
55
50
Hum_Control
Hum_GWI
Sample Group
Hum_Control
Hum_GWI

Fig. 4

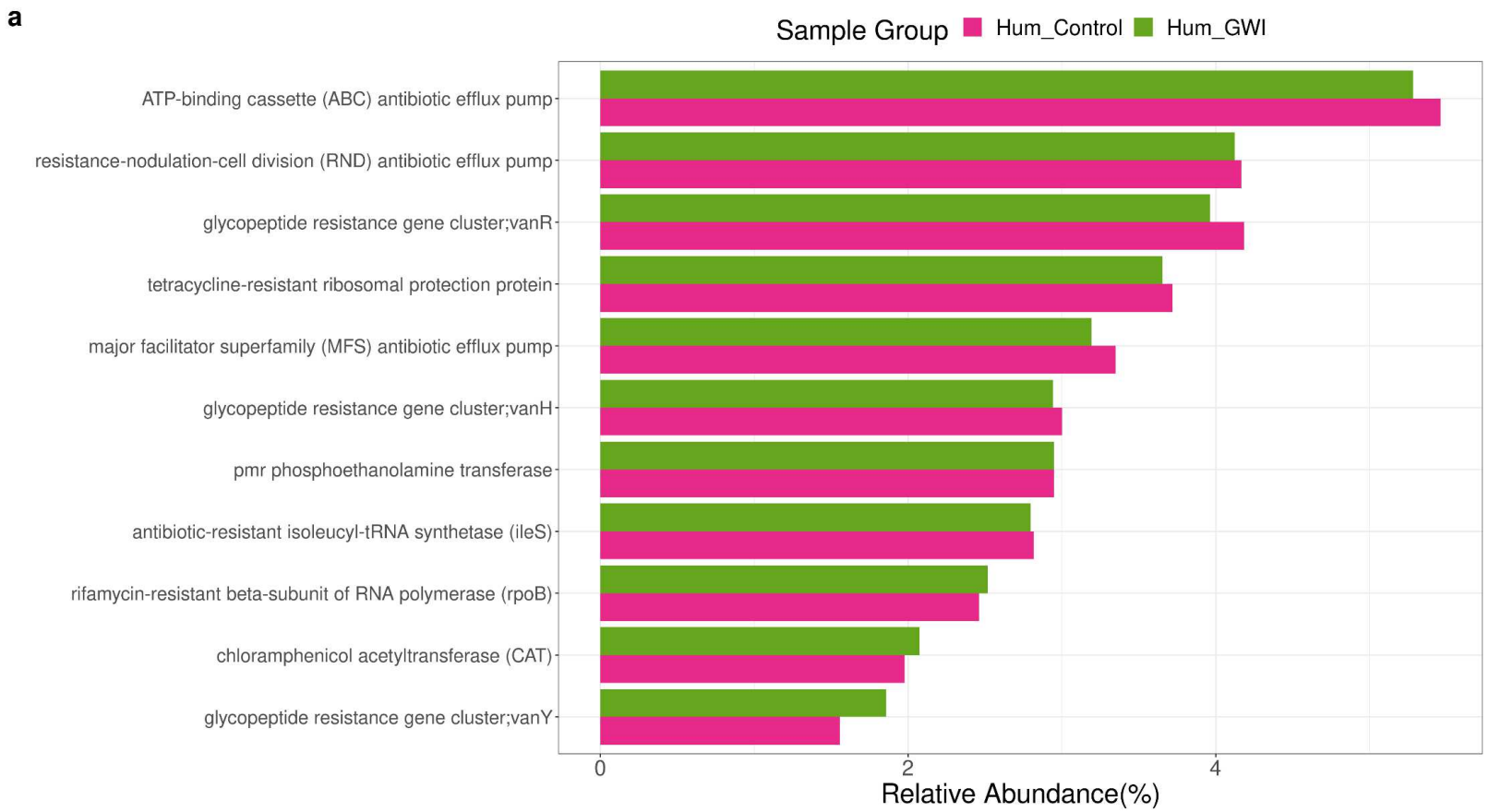
a
Sample Group
Hum_Control
Hum_GWI
ATP-binding cassette (ABC) antibiotic efflux pump
resistance-nodulation-cell division (RND) antibiotic efflux pump
glycopeptide resistance gene cluster;vanR
tetracycline-resistant ribosomal protection protein
major facilitator superfamily (MFS) antibiotic efflux pump
glycopeptide resistance gene cluster;vanH
pmr phosphoethanolamine transferase
antibiotic-resistant isoleucyl-tRNA synthetase (ileS)
rifamycin-resistant beta-subunit of RNA polymerase (rpoB)
chloramphenicol acetyltransferase (CAT)
glycopeptide resistance gene cluster;vanY
0
2
4
Relative Abundance(%)

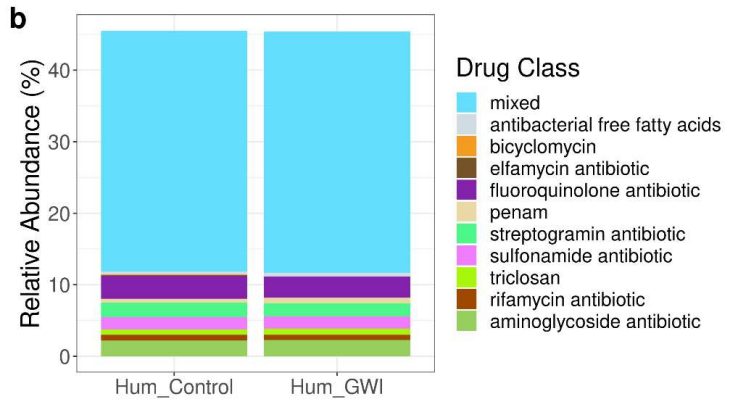
b
Relative Abundance (%)
0
10
20
30
40
Hum_Control
Hum_GWI
Drug Class
mixed
antibacterial free fatty acids
bicyclomycin
elfamycin antibiotic
fluoroquinolone antibiotic
penam
streptogramin antibiotic
sulfonamide antibiotic
triclosan
rifamycin antibiotic
aminoglycoside antibiotic

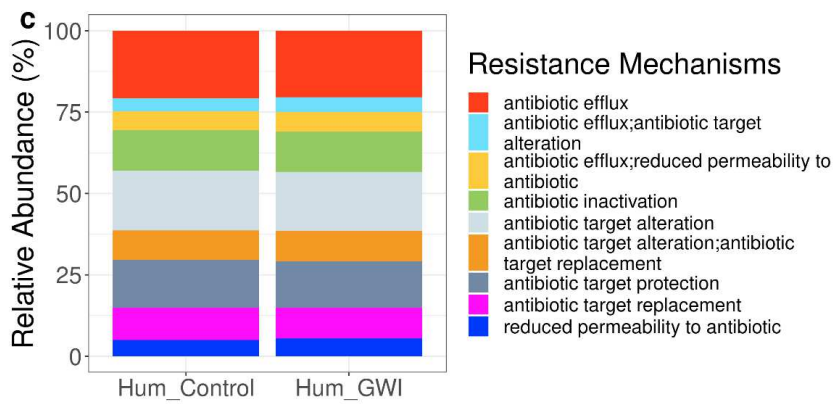
c
Relative Abundance (%)
0
25
50
75
100
Hum_Control
Hum_GWI
Resistance Mechanisms
antibiotic efflux
antibiotic efflux;antibiotic target alteration
antibiotic efflux;reduced permeability to antibiotic
antibiotic inactivation
antibiotic target alteration
antibiotic target alteration;antibiotic target replacement
antibiotic target protection
antibiotic target replacement
reduced permeability to antibiotic

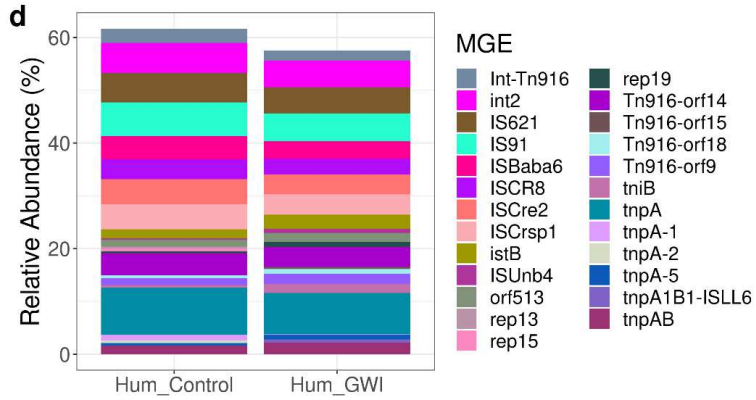
d
Relative Abundance (%)
0
20
40
60
Hum_Control
Hum_GWI
MGE
Int-Tn916
int2
IS621
IS91
ISBaba6
ISCR8
ISCre2
ISCrsp1
istB
ISUnb4
orf513
rep13
rep15
rep19
Tn916-orf14
Tn916-orf15
Tn916-orf18
Tn916-orf9
tniB
tnpA
tnpA-1
tnpA-2
tnpA-5
tnpA1B1-ISLL6
tnpAB

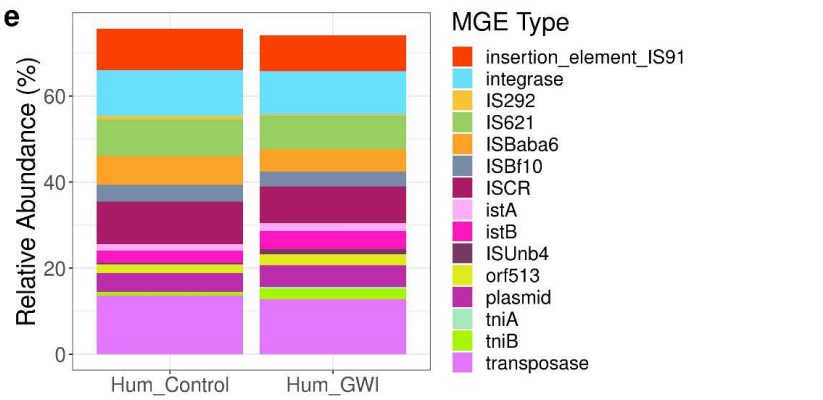
e
Relative Abundance (%)
0
20
40
60
Hum_Control
Hum_GWI
MGE Type
insertion_element_IS91
integrase
IS292
IS621
ISBaba6
ISBf10
ISCR
istA
istB
ISUnb4
orf513
plasmid
tniA
tniB
transposase

Fig. 5

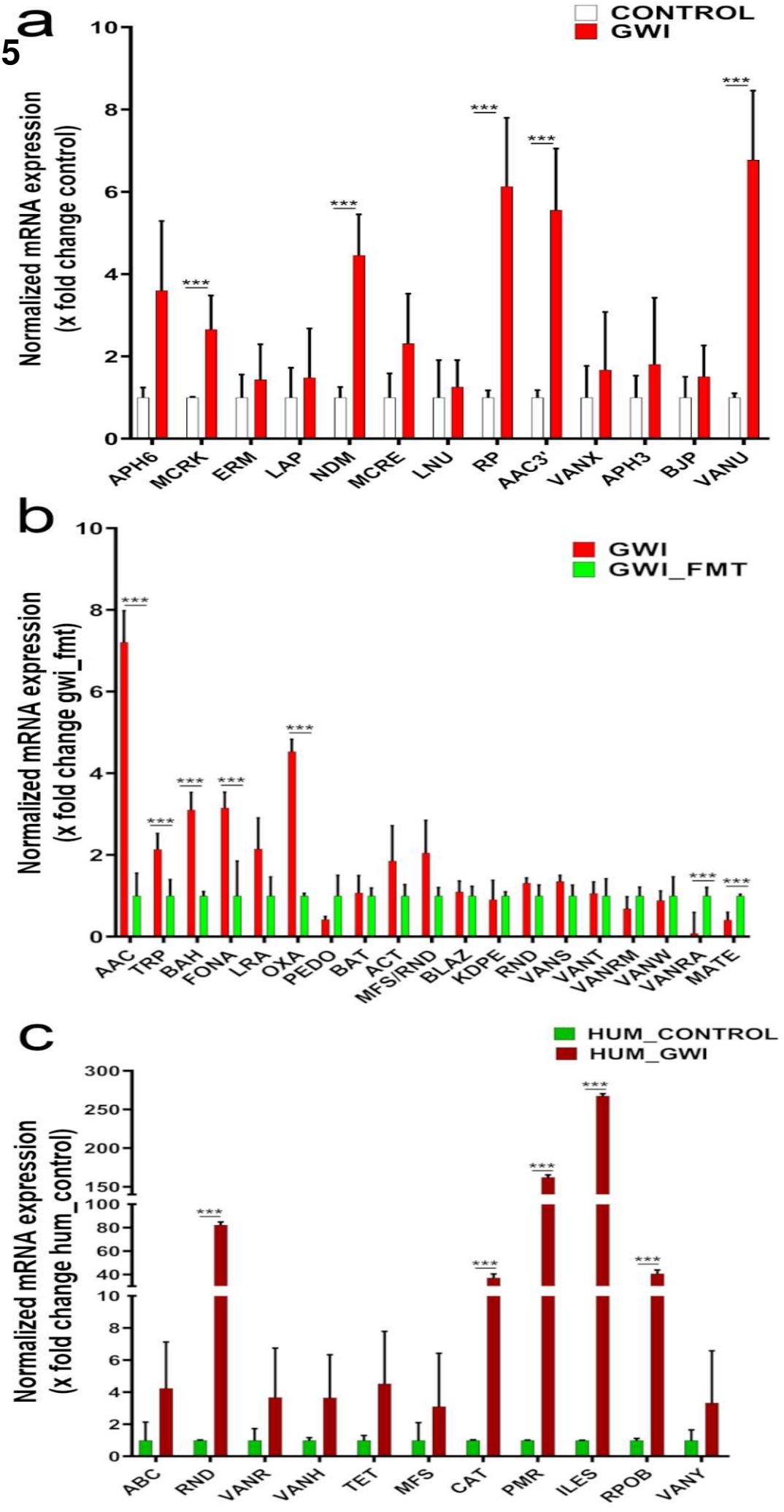
a
CONTROL
GWI
Normalized mRNA expression
(x fold change control)
APH6
MCRK
ERM
LAP
NDM
MCRE
LNU
RP
AAC3'
VANX
APH3
BJP
VANU
b
GWI
GWI_FMT
Normalized mRNA expression
(x fold change gwi_fmt)
AAC
TRP
BAH
FONA
LRA
OXA
PEDO
BAT
ACT
MFS/RND
BLAZ
KDPE
RND
VANS
VANT
VANRM
VANW
VANRA
MATE
c
HUM_CONTROL
HUM_GWI
Normalized mRNA expression
(x fold change hum_control)
ABC
RND
VANR
VANH
TET
MFS
CAT
PMR
ILES
RPOB
VANY

Fig. 6

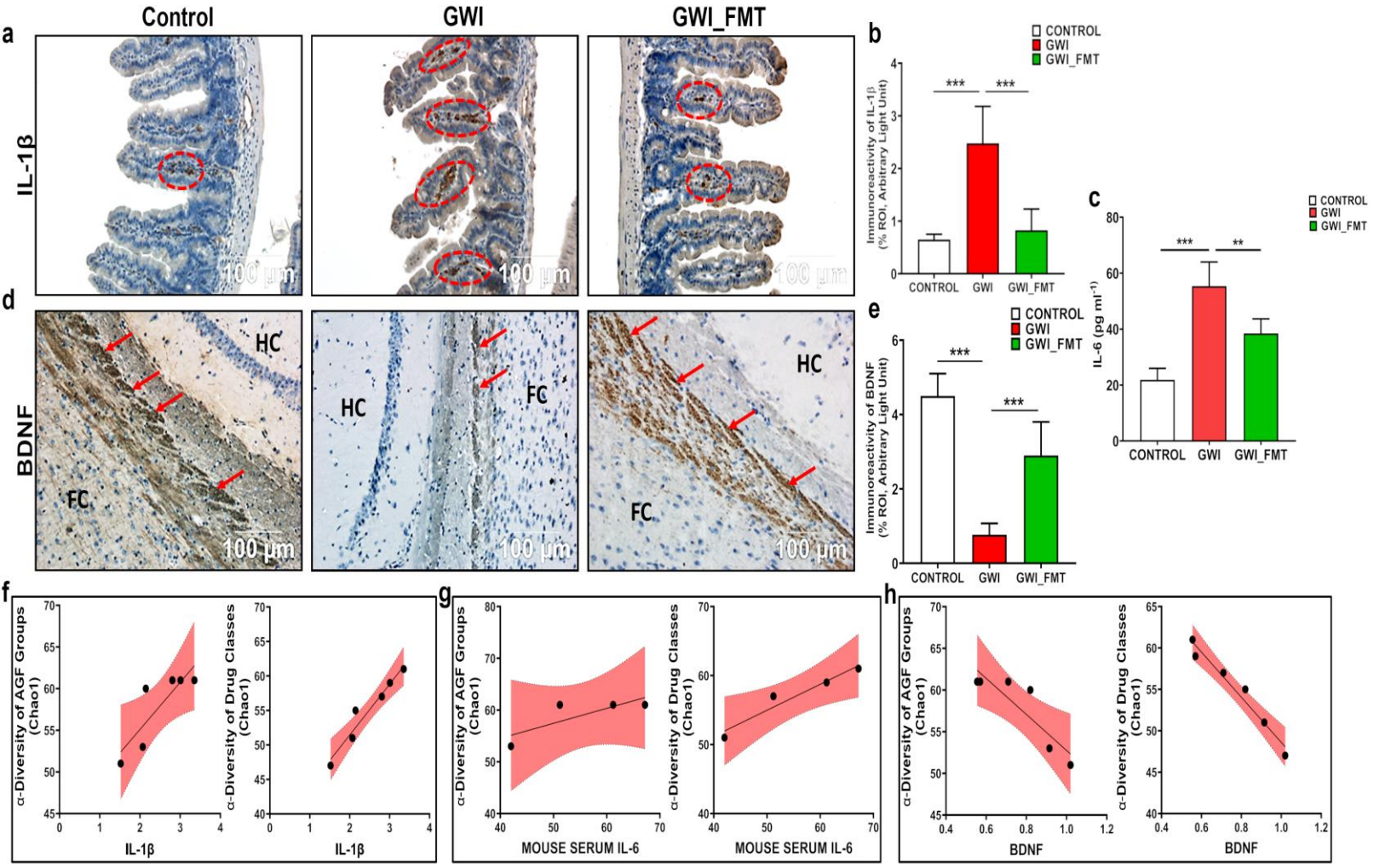
Control
GWI
GWI_FMT
a
IL-1β
100 μm
b
CONTROL
GWI
GWI_FMT
***
***
Immunoreactivity of IL-1β (% ROI, Arbitrary Light Unit)
c
**
IL-6 (pg ml⁻¹)
d
BDNF
HC
FC
e
Immunoreactivity of BDNF (% ROI, Arbitrary Light Unit)
f
α-Diversity of AGF Groups (Chao1)
α-Diversity of Drug Classes (Chao1)
IL-1β
g
MOUSE SERUM IL-6
h
BDNF

List of primers for Real time PCR analysis:

a. CONTROL and GWI:

SL no.	Gene name	Abbreviation	Forward	Reverse	Ta
1	General Bacterial Porin with reduced permeability to beta-lactams GBP R/P	GBP	TAACGATCAGCTTGGTGCTG	CTTTGAAAGCACCGTTGTCA	56.3
2	APH(3') R/P	APH(3')	GCATCAGGCTCTTTCACTCC	CGGCCAGATCGTTATTCAGT	55.7
3	MCR phosphoethanolamine transferase MCR_R/P	MCRK/E	AAATTGGCGAGTACGACACC	GCTCGTCCTGGGTGTTTTTA	56.3
4	rifampin phosphotransferase RP_R/P	RP	TTCGGACTTGGAGAAGCACT	GTCCGTAGATCGCCAATGTT	56
5	glycopeptide resistance gene cluster;vanU	vanU	TCGTGAGGCTGTTGGAGTAA	TCGCCAAAATCACAATTCAA	55.8
6	methicillin resistant PBP2	PBP2	GCTCAAATCGGTTGGTTTGT	CTCGGCAAACTTTCTTGCAT	56.2
7	APH(6)	APH(6)	ATCGCTTTGCAGCTTTGTTT	ATGATGCAGATCGCCATGTA	56.2
8	BJP beta-lactamase	BJP	TCAAGCTCATCCTCAACACG	TTTTCTCGTCACCCGGATAG	55.9
9	lipid A phosphatase LAP	LAP	GCGTACTCATCTGCGATCAA	GCCGTAGACCGTCTTCACAT	56.1
10	AAC(3)	AAC(3)	ATAGCGGCCGAGTCTTGTTA	GAGGATCGGTTGTTCGTAGG	55.5
11	NDM beta-lactamase	NDM	ATATCACCGTTGGGATCGAC	TAGTGCTCAGTGTCGGCATC	56
12	lincosamide nucleotidyltransferase (LNU)	LNU	AGCGTTCAAACCAAGCAAGT	CTGAGCAGCAACTTCACTCG	55.9
13	glycopeptide resistance gene cluster;vanX	vanX	TGCTCTTATGGGACGGCTAC	AAGCCACATACCCTTTCGTG	56.5
14	Erm 23S ribosomal RNA methyltransferase ERM	ERM	AATTGTGGATCAGGCAAAGG	ATTCCACTGCGAGCACTCTT	56.1

b. GWI and GWI_FMT:

SL no.	Gene name	Abbreviation	Forward	Reverse	Ta
1	glycopeptide resistance gene cluster;vanRA	VAN RA	CAGTGGAGTAAAGGAGCAGAAC	TCGGTGGGAGTAAGGGATAA	54.6
2	glycopeptide resistance gene cluster;vanRM	VAN RM	GTCAAGTCCGTGCACAGTATAA	GTTCACACGAGCAACCAATTC	55.3
3	glycopeptide resistance gene cluster;vanS	VANS	TCACGTTGGACAAAGCGTATC	GGTCATCTGCACCAGCATATAG	56.5
4	major facilitator superfamily (MFS) antibiotic efflux pump;resistance-nodulation-cell division (RND) antibiotic efflux pump	MFS/RND	AACTCGCCGCGTCAATATAA	GGCCAGGTTTCCTGTATCAA	56.1
5	glycopeptide resistance gene cluster;vanT	VANT	ATACCGCCGATACGGATAGA	TAAATGTGAATTGATGGCGGTT	56.7
6	kdpDE	KDPE	CAGGCTATTCGTCGCTTTCT	GGCCGAGATCGAGAATAATCAA	56.7
7	multidrug and toxic compound extrusion (MATE) transporter	MATE	CCGCTGAATTTCGGCATTATC	CGACAAACATTTGCGTCAGTAG	58.3
8	blaZ beta-lactamase	BLAZ	TGCGTCTTGATCGGGAATTAG	CTTAACGAACCCACTGCATAGT	56.6
9	General Bacterial Porin with reduced permeability to beta-	RND	GTCACTGGAGAAAGTGTCAGAGC	AATACATCCGCAGCCGTAAG	56.3

	lactams;resistance-nodulation-cell division (RND) antibiotic efflux pump				
10	AAC(6')	AAC (6')	CAACTGTCCAAGATCCACCA	CCCGACAGCTTGATCCTCTA	56.1
11	OXA beta-lactamase	OXA	GTGTACCTCACCTGTTTCATCT	TGACCACGCTGAATCACTAAA	54.1
12	Bah amidohydrolase	BAH	GAAGGACCAACGGCAATACA	GGTCGTCTGCGAATCGTAATAA	57.2
13	FONA beta-lactamase	FONA	ACACGGCGATGAACAAGAT	ACGCTTATCACCTGGAATGG	56
14	tunicamycin resistance protein	TRP	CAGAAGGCTGAACCCATCTTAC	TTGAACGCCCGCCATAAA	57.9
15	subclass B3 PEDO beta-lactamase	PEDO	TGACCACACAGGCACATTAC	CCTTCATCACACTGGCATCTT	55.7
16	class C LRA beta-lactamase;class D LRA beta-lactamase	LRA	GCGATTCGGTCGTATGGTATT	ATGCTCAGGCCGTCATTT	55.9
17	ACT beta-lactamase	ACT	CCTTATTCGAGCTGGGTTCTAT	GTCAGCTCAGGCCAGTATTT	53.5
18	BAT Beta-lactamase	BAT	GCTTACAAGTAGGAGCTGTAGAAG	CGGGCCATCGCTTGATAATA	54

c. CONTROL and GWI veterans:

SL no.	Gene name	Abbreviation	Forward	Reverse	Ta
1	ATP-binding cassette (ABC) antibiotic efflux pump	ABC	GAAGGGCCACAAAGAAGTATTG	CAGAGATGGAAGAGGCTGAAA	55.8
2	glycopeptide resistance gene cluster;vanR	VANR	CACTTCTGCCGGAGGATTT	GTTAAGGTTCTGCCTTTGTTCTG	55.9
3	resistance-nodulation-cell division (RND) antibiotic efflux pump	RND	GATCCTGACTCCAGCTCTTTG	CTCTTCTCGAACATGCGGTTA	55.8
4	tetracycline-resistant ribosomal protection protein	TET	CCTGTCCGGGAGAAATTGTTAT	CTCTACCGTTGTCCGAAGTAATG	56.9
5	major facilitator superfamily (MFS) antibiotic efflux pump	MFS	GCAAATGCGGAGACTCAAAC	CCCTATCGCTACGGCAATAAT	56.6
6	pmr phosphoethanolamine transferase	PMR	CTCGGTGGTTATTCCCGTTTAT	CAGCAGGATCTCATACTCTTTCC	56.1
7	glycopeptide resistance gene cluster;vanH	VANH	GCTTTGATGCTGATGCTGATG	GTCATATCCCGCAGCTCTTT	56.8
8	antibiotic-resistant isoleucyl-tRNA synthetase (ileS)	ILESH	CCTACTACTTCTTCACGCTGTATG	CAGCAGGTAACGATCCATCTC	54.7
9	rifamycin-resistant beta-subunit of RNA polymerase (rpoB)	RPOBH	ACCTTCTCCGATCCGTACTT	CACGGTCTGGGACTTGATTT	55.1
10	chloramphenicol acetyltransferase (CAT)	CATH	CAGGTAAAGAACCCGAACATCA	TGCGATCTGGCAAGAGAAAG	56.4